Article

Molecular Cell

USP1 Is Required for Replication Fork Protection in BRCA1-Deficient Tumors

Graphical Abstract

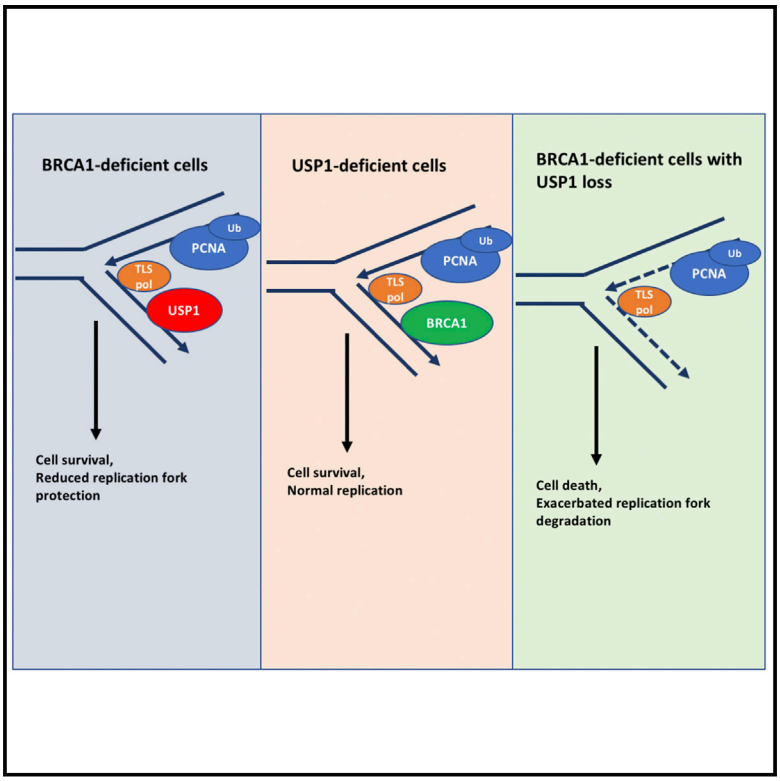

Authors

Kah Suan Lim, Heng Li, Emma A. Roberts, ..., Timur Yusufzai, Ning Zheng, Alan D. D'Andrea

Correspondence

alan_dandrea@dfci.harvard.edu

In Brief

Lim et al. identify a key function of a deubiquitinating enzyme, USP1, in replication in BRCA1-deficient tumors. USP1 localizes to replication forks and promotes their stabilization in BRCA1-deficient cells. Loss of USP1 results in reduced cell survival and replication fork degradation, suggesting that USP1 inhibitors may be useful in treating BRCA1-deficient tumors.

Highlights

- USP1 is significantly upregulated in BRCA1-deficient tumors
- Loss of USP1 and BRCA1 is synthetic lethal
- USP1 directly binds to and stabilizes the replication fork in BRCA1-deficient cells
- Synthetic lethality between USP1 and BRCA1 is due to persistent monoubiquitinated PCNA

Lim et al., 2018, Molecular Cell 72, 925–941
December 20, 2018
https://doi.org/10.1016/j.molcel.2018.10.045

CellPress

Molecular Cell
Article

USP1 Is Required for Replication Fork Protection in BRCA1-Deficient Tumors

Kah Suan Lim,[1] Heng Li,[3] Emma A. Roberts,[1] Emily F. Gaudiano,[1] Connor Clairmont,[1] Larissa Alina Sambel,[1,2] Karthikeyan Ponnienselvan,[1] Jessica C. Liu,[1] Chunyu Yang,[1,2] David Kozono,[1] Kalindi Parmar,[1,2] Timur Yusufzai,[1] Ning Zheng,[3,4] and Alan D. D'Andrea[1,2,5,*]

[1]Department of Radiation Oncology, Dana-Farber Cancer Institute, Boston, MA 02215, USA
[2]Center for DNA Damage and Repair, Dana-Farber Cancer Institute, Boston, MA 02215, USA
[3]Department of Pharmacology, University of Washington, Seattle, WA 98195, USA
[4]Howard Hughes Medical Institute, Box 357280, Seattle, WA, USA
[5]Lead Contact
*Correspondence: alan_dandrea@dfci.harvard.edu
https://doi.org/10.1016/j.molcel.2018.10.045

SUMMARY

BRCA1-deficient tumor cells have defects in homologous-recombination repair and replication fork stability, resulting in PARP inhibitor sensitivity. Here, we demonstrate that a deubiquitinase, USP1, is upregulated in tumors with mutations in BRCA1. Knockdown or inhibition of USP1 resulted in replication fork destabilization and decreased viability of BRCA1-deficient cells, revealing a synthetic lethal relationship. USP1 binds to and is stimulated by fork DNA. A truncated form of USP1, lacking its DNA-binding region, was not stimulated by DNA and failed to localize and protect replication forks. Persistence of monoubiquitinated PCNA at the replication fork was the mechanism of cell death in the absence of USP1. Taken together, USP1 exhibits DNA-mediated activation at the replication fork, protects the fork, and promotes survival in BRCA1-deficient cells. Inhibition of USP1 may be a useful treatment for a subset of PARP-inhibitor-resistant BRCA1-deficient tumors with acquired replication fork stabilization.

INTRODUCTION

BRCA1 and *BRCA2* are frequently mutated or silenced due to epigenetic changes in breast and ovarian cancers, providing an opportunity for targeted therapy (Farmer et al., 2005). Proteins encoded by *BRCA1* and *BRCA2* genes are master regulators of genomic stability and are essential for accurate DNA double-strand break (DSB) repair by homologous recombination (HR) (Gudmundsdottir and Ashworth, 2006). BRCA1 is required for C-terminal binding protein 1 (CtBP1) interacting protein (CtIP)-mediated resection of DSBs to generate recombinogenic single-strand DNA (ssDNA) through the Mre11-Rad50-Nbs1 (MRN) complex (Moynahan et al., 1999; Yun and Hiom, 2009). BRCA2 facilitates subsequent loading of RAD51 on ssDNA and promotes HR (Moynahan et al., 2001; Thorslund et al., 2010). BRCA1 and BRCA2 are also required for the protection of stalled replication forks by limiting nucleolytic degradation (Lomonosov et al., 2003; Pathania et al., 2014; Schlacher et al., 2011, 2012).

Poly (ADP-ribose) polymerase (PARP) inhibitors have had significant success in improving progression-free survival in BRCA1- or BRCA2-deficient ovarian tumors (Ledermann et al., 2014, 2016; Lord and Ashworth, 2017; Oza et al., 2015) and remain the only US Food and Drug Administration (FDA)-approved "synthetic lethal" therapeutic agents for BRCA1- or BRCA2-deficient tumors. However, therapeutic resistance to PARP inhibitors has emerged, resulting from either restoration of HR or replication fork stabilization (Bunting et al., 2010; Ray Chaudhuri et al., 2016; Rondinelli et al., 2017; Xu et al., 2015). There is a critical need for a specific class of drugs that can target BRCA1- or BRCA2-deficient tumors and potentially overcome PARP inhibitor resistance.

Recent studies indicated that protein ubiquitination at the replication fork regulates fork stability (Chu et al., 2015; Elia et al., 2015; Lecona et al., 2016). Protein ubiquitination is a critical post-translational modification that regulates multiple cellular processes. Protein ubiquitination is controlled by the coordinate activity of ubiquitin E3 ligases and deubiquitinating enzymes (DUBs) (D'Andrea and Pellman, 1998; Komander and Rape, 2012). DUBs cleave the isopeptide bond between ubiquitin and the modified protein. Over 100 DUBs are known, and these proteins are subdivided into six subfamilies (Davis and Simeonov, 2015; Nijman et al., 2005b). The USP (ubiquitin-specific protease) subfamily is the largest subfamily, with 58 members. USPs are cysteine proteases, containing a highly conserved catalytic domain. The generation of small-molecule inhibitors of USPs is currently an active pursuit of the pharmacology industry (Davis and Simeonov, 2015).

The function and regulation of USP1, a member of the USP subclass of DUBs, has been evaluated in considerable detail. USP1 regulates the Fanconi anemia (FA) DNA repair pathway, and USP1-deficient cells or mice exhibit FA phenotypes (Kim et al., 2009; Nijman et al., 2005a; Oestergaard et al., 2007). Like two closely related DUBs, USP12 and USP46, USP1 binds to a conserved WD40-repeat protein, UAF1 (Cohn et al., 2009; Cohn et al., 2007; Sowa et al., 2009). Other USPs have

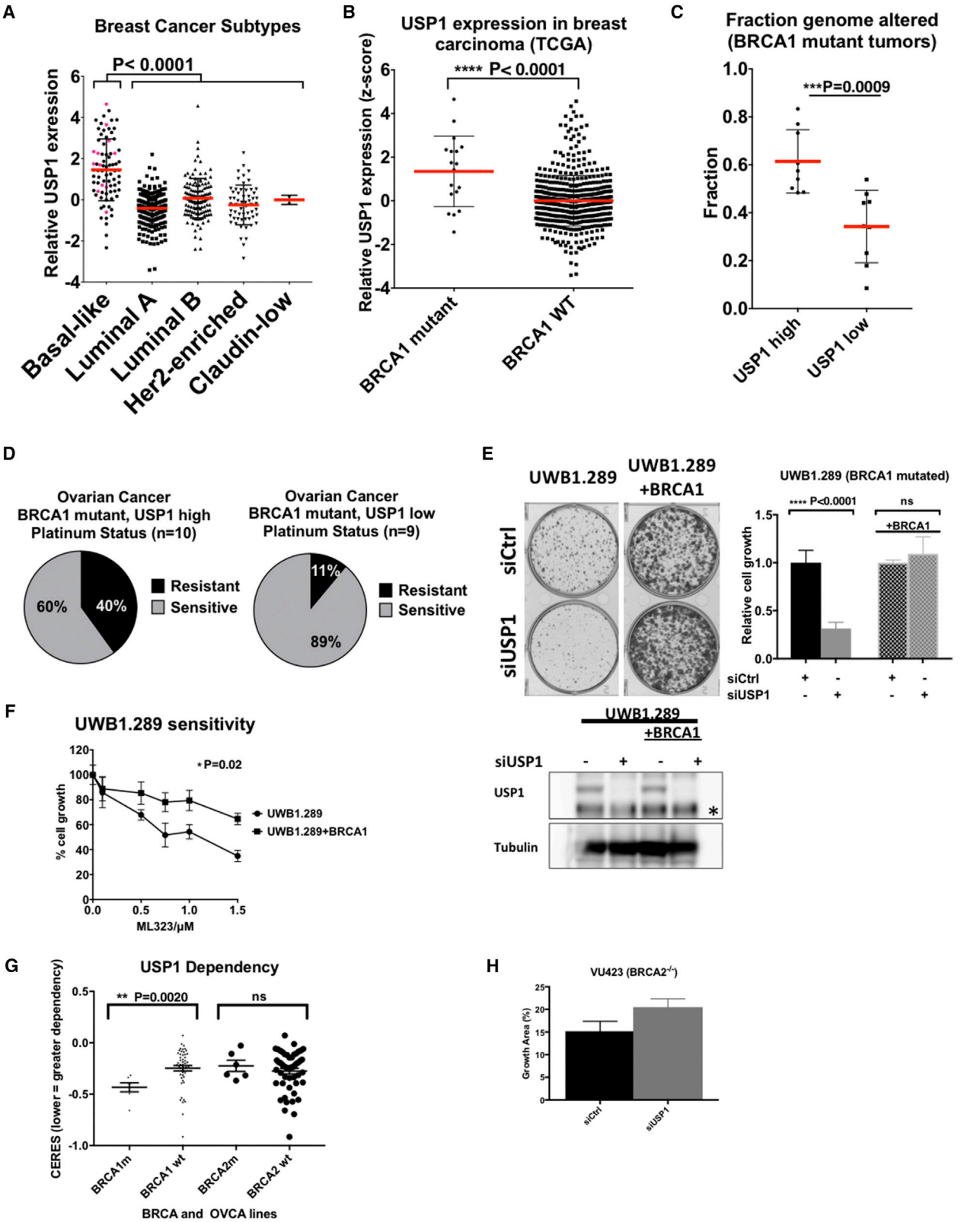

(legend on next page)

WD40-repeat binding partners, suggesting a more general mechanism of USP activation (Villamil et al., 2013). USP1, USP12, and USP46 exist in a mostly inactive state, and their isopeptidase activity is stimulated by UAF1 binding. Recent crystallographic studies demonstrate that UAF1 binds to a distinct site on USP12 or USP46 and, through an allosteric interaction, stimulates DUB activity (Li et al., 2016; Yin et al., 2015). The UAF1-binding site of USP1, USP12, and USP46 is the zinc-finger region, at the tips of the DUB finger structure, distant (40 Å) from the catalytic triad of the protease (Li et al., 2016; Ye et al., 2009). The crystal structure of USP1 has not been solved; however, it is a larger protein, suggesting that there may be additional regulatory regions in USP1 not present in USP12 or USP46. USP12 and USP46, but not USP1, are also activated independently by another WD40-repeat protein (WDR20) through an additional allosteric site (Kee et al., 2010; Li et al., 2016).

Recent studies suggest that the USP1-UAF1 complex has a direct interaction with DNA. First, the known substrates of USP1-UAF1 include FANCD2-Ubiquitin (Ub), FANCI-Ub, and proliferating cell nuclear antigen (PCNA)-Ub, all of which are DNA-binding proteins (Huang et al., 2006; Nijman et al., 2005a). Second, USP1-UAF1 travels with the replication fork during DNA synthesis, suggesting that it removes ubiquitin from protein substrates residing at the fork (Dungrawala et al., 2015). Interestingly, the hydroxyurea-induced increase in FANCD2-Ub and PCNA-Ub at the fork correlates temporally with the release of USP1-UAF1 from the fork (Dungrawala et al., 2015), suggesting that reduced local expression of USP1 accounts in part for the upregulated monoubiquitination of these substrates. Third, UAF1 has been shown to have DNA-binding activity and directly interact with the HR protein RAD51AP1 (Cukras et al., 2016; Liang et al., 2016). Whether USP1 also has DNA-binding activity or a role in replication fork protection remains unknown.

In the current study, we identified a function of USP1 during replication in BRCA1-deficient cells. USP1 binds to DNA independently of UAF1 and is stimulated preferentially by DNA structures mimicking a replication fork. An internally truncated version of USP1 (USP1-Trunc), which has active deubiquitinating activity, neither binds to DNA nor is stimulated by DNA. While wild-type USP1 localizes to replication forks of transfected human cells, mutant USP1-Trunc fails to localize to and stabilize the replication fork. USP1 is required for stabilization of the replication fork of BRCA1-deficient cells, and knockout or small-molecule inhibition (Liang et al., 2014) with a specific inhibitor of the USP1-UAF1 complex is synthetic lethal in these cells.

While a USP1 substrate, FANCD2, had previously been shown to have a replication fork protective role (Kais et al., 2016; Schlacher et al., 2012), we found that a different USP1 substrate, PCNA, is important in replication fork protection in BRCA1-deficient cells. Synthetic lethality between USP1 and BRCA1 was rescued by silencing either the PCNA ubiquitin ligase RAD18 or the translesion synthesis (TLS) polymerase POLK, which accumulates following USP1 silencing, due to the persistence of Ub-PCNA. Our results suggest that accumulation of TLS polymerases leads to enhanced replication fork instability in BRCA1-deficient cells and provides a mechanism of synthetic lethality in BRCA1-deficient cells. Moreover, a USP1 inhibitor can kill a subset of BRCA1-deficient cells that have acquired PARP inhibitor resistance due to replication fork stabilization. In addition, our data suggest a potential role of the BRCA1 protein in mitigating replication fork instability resulting from aberrant TLS. USP1 inhibitors thus represent a class of inhibitors with potential therapeutic use in BRCA1-deficient cancers.

RESULTS

USP1 Is Overexpressed in BRCA1-Deficient Tumors

Using published data from The Cancer Genome Atlas (TCGA) breast cancer consortium (http://www.cbioportal.org) and GEO database GDS2250, we found that USP1 was significantly overexpressed in HR-deficient basal-like breast cancers compared to the other breast cancer subtypes ($p < 0.0001$) (Figures 1A and S1A) (Cancer Genome Atlas Network, 2012). USP1 overexpression correlated with BRCA1 deficiency in breast tumors ($p < 0.0001$) (Figure 1B). BRCA1-deficient tumors with high expression of USP1 have a higher level of genome alterations (Figure 1C). A similar correlation was observed in BRCA1-deficient ovarian tumors (Figure S1B). Interestingly, USP1 expression was also enriched in platinum-resistant ovarian cancers with BRCA1 mutation (Figure 1D). Overexpression of USP1 was higher in breast cancers than in other cancer types (Figure S1C).

Figure 1. USP1 Is Overexpressed in HR-Deficient Tumors

(A) USP1 mRNA levels in HR-deficient basal-like breast cancers were plotted against other breast cancer subtypes using data from TCGA.

(B) USP1 mRNA levels in BRCA1 mutated or BRCA1 wild-type breast cancers were plotted using data from TCGA.

(C) Fraction of genome altered in BRCA1 mutant breast cancers with high USP1 expression levels or low USP1 expression levels were plotted using data from TCGA.

(D) Platinum sensitivity status of BRCA1 mutant ovarian cancers with high USP1 expression levels or low USP1 expression levels was graphed using data from TCGA.

(E) Top left: representative images of the colonies of BRCA1-mutated UWB1.289 and its isogenic BRCA1-reconstituted UWB1.289+BRCA1 cells with either control siRNA (siCtrl) or siUSP1 in a clonogenic assay. Bottom left: western blot of the lysates from UWB1.289 and UWB1.289+BRCA1 cells following USP1 silencing (asterisk indicates a nonspecific band). Right: graphical quantification of a clonogenic assay of UWB1.289 and UWB1.289+BRCA1 cells following treatment with either control siRNA or USP1 siRNA (n = 5).

(F) Dose-response graph of UWB1.289 and UWB1.289+BRCA1 cells treated with a USP1 inhibitor, ML323 (n = 6). Values are mean ± SEM.

(G) CRISPR gene-knockout effects inferred by the CERES computational method were compared in 57 breast and ovarian cancer cell lines grouped by BRCA1 or BRCA2 mutation status using data from the Broad Institute Cancer Dependency Map and Cancer Cell Line Encyclopedia. Error bars reflect mean ± SEM. CERES values for wild-type versus mutant cell lines were compared via the Mann-Whitney *U* test.

(H) Quantitation of growth of BRCA2-deficient VU423 cells after USP1 silencing (n = 2).

See also Figure S1.

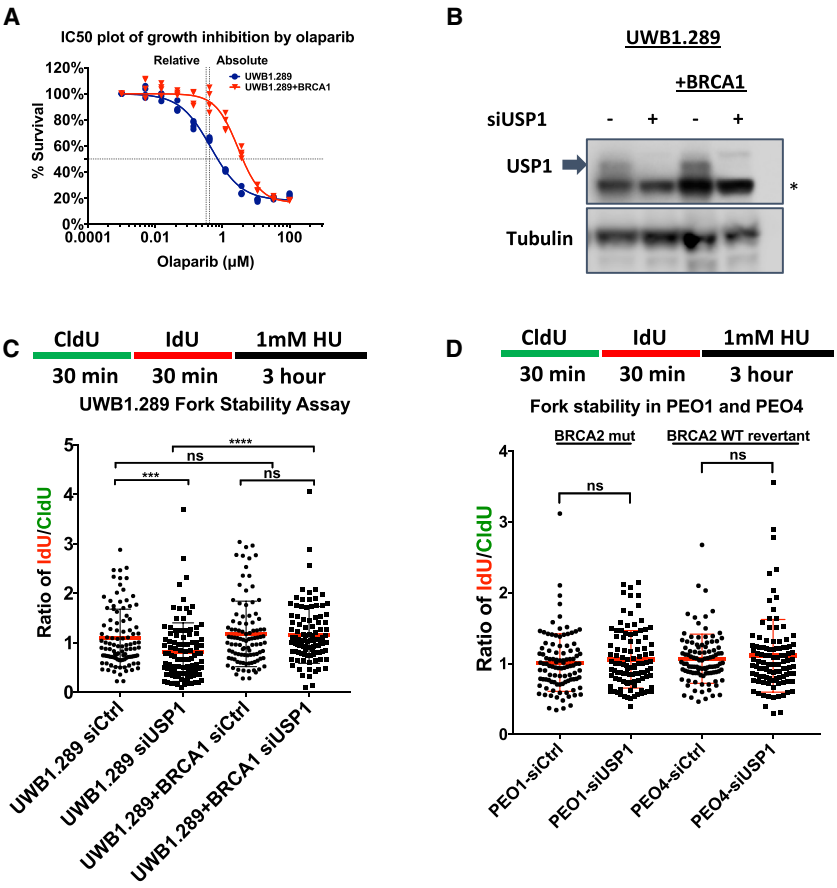

Figure 2. USP1 Silencing Causes Replication Fork Instability in BRCA1-Deficient Cells

(A) Half maximal inhibitory concentration (IC_{50}) plots of UWB1.289 and UWB1.289+BRCA1 cells for survival after olaparib treatment showing a functional rescue of BRCA1 in the reconstituted UWB1.289 cells. The IC_{50} values for olaparib in UWB1.289 cells and UWB1.289+BRCA1 cells were 0.45 μM and 2.95 μM, respectively.

(B) Western blot of the lysates from UWB1.289 and UWB1.289+BRCA1 cells following USP1 silencing (asterisk indicates a nonspecific band).

(C) Schematic of 5-chloro-2′-deoxyuridine (CldU), 5-iodo-2′-deoxyuridine (IdU), and hydroxyurea (HU) treatment (top) and graphical quantification of fiber assay measuring fork degradation in UWB1.289 and UWB1.289+BRCA1 cells following USP1 silencing (bottom). The median values for UWB1.289 siCtrl, siUSP1, UWB1.289+BRCA1 siCtrl, and UWB1.289+BRCA1 siUSP1 are 1.442, 1.074, 1.407, and 1.455 respectively. Statistical analysis was performed on at least 100 cells per condition. The fiber assays were repeated twice, and the data from a representative experiment are shown.

(D) Schematic of CldU, IdU, and hydroxyurea treatment (top) and quantification of fork stability in PEO1 (BRCA2 mutant) and PEO4 (BRCA2 revertant) cells following USP1 silencing (bottom). The median values for PEO1 siCtrl, PEO1 siUSP1, PEO4 siCtrl, and PEO4 siUSP1 are 0.972, 0.979, 1.006, and 1.027. The fiber assay was repeated three times with at least 100 fibers per condition, and the data from a representative experiment are shown.

See also Figure S2.

USP1 was also the highest expressed of all its orthologs in breast cancers (Figure S1D). Of the top USP1-overexpressing breast tumors, BRCA1 was the second most commonly mutated gene (Figure S1E).

We further evaluated the synthetic lethal relationship between BRCA1 and USP1 in a BRCA1 mutant ovarian cancer cell line, UWB1.289. Silencing USP1 by small interfering RNA (siRNA) transfection resulted in reduced growth of UWB1.289, but not of UWB1.289+BRCA1, complemented cells (Figure 1E). Inhibition of USP1 activity by treatment of UWB1.289 cells with a specific DUB inhibitor of USP1, ML323 (Liang et al., 2014), also resulted in reduced growth of UWB1.289 cells compared to UWB1.289+BRCA1 cells (Figures 1F and S1F). Synthetic lethality between USP1 and BRCA1 was also evident in another cancer cell line using an *in vivo* mouse xenograft model (Figure S1G). BRCA1-deficient MDA-MB-436 breast cancer cells with clustered regularly interspaced short palindromic repeats (CRISPR)-mediated knockout of USP1 exhibited significantly reduced tumor growth in athymic nude mice compared to MDA-MB-436 cells with reconstitution of BRCA1 (Figure S1G). A cancer dependency study from the Broad Institute also confirmed that BRCA1-deficient, but not BRCA2-deficient, breast and ovarian cell lines are hyperdependent on USP1 for survival (Figure 1G). Depletion of USP1 also did not affect the growth of BRCA2-deficient VU423 cells (Figure 1H).

USP1 Protects Replication Forks in BRCA1-Deficient Cells

BRCA1-deficient cells are defective in replication fork stabilization and are dependent on FANCD2 for fork protection and restart (Kais et al., 2016). Since USP1 regulates the levels of FANCD2 monoubiquitination, we examined the role of USP1 in replication fork protection in BRCA1-deficient cells. Functional complementation of BRCA1 was confirmed by PARP inhibitor resistance in UWB1.289+BRCA1 cells (Yazinski et al., 2017) (Figure 2A). We used a low dose of hydroxyurea (1 mM) that does not lead to replication fork instability in BRCA1-deficient cells. Hydroxyurea treatment of BRCA1-deficient cells for 3 hr did not result in replication fork instability (Figures 2B, 2C, and S2A). Silencing of USP1 in HeLa cells also had no significant effect on hydroxyurea-mediated fork stalling and degradation; however, silencing of USP1 and BRCA1 led to a significantly higher level of fork degradation after hydroxyurea treatment (Figure S2A). Similarly, knockdown of USP1 in BRCA1-deficient UWB1.289 cells resulted in enhanced fork degradation after stalling with hydroxyurea (Figures 2B and 2C). In contrast, knockdown of USP1 in the BRCA1-complemented UWB1.289 cells did not enhance fork degradation (Figures 2B and 2C). Treatment of BRCA1 deficient MDA-MB-436 cells with the USP1 inhibitor ML323 also resulted in enhanced fork degradation following hydroxyurea treatment, and this effect is not increased with USP1 silencing (Figure S2B). Loss of USP1 in BRCA2-deficient PEO1 ovarian

cancer cells did not lead to a decrease in replication fork stability (Figure 2D). Interestingly, while loss of USP1 in BRCA1-proficient HeLa cells did not lead to a decrease in fork stability, it reduced the efficiency of fork progression after restart following hydroxyurea (HU) treatment (Figure S2C). Taken together, these results indicate that USP1 promotes replication fork stabilization in BRCA1-deficient, but not BRCA2-deficient, cells and suggests that USP1 is upregulated in BRCA1-deficient cells in order to enhance fork protection. Consistent with the role of USP1 in stabilizing the replication fork, many genes encoding proteins involved in fork stability were among the top 20 genes whose expression correlated with USP1 expression in breast and ovarian cancers (Figure S2D). Also, siRNA knockdown of USP1 in BRCA1-deficient retinal pigment epithelial (RPE) cells resulted in increased chromosomal breaks and aberrations (Figure S2E).

USP1 Is a DNA-Binding Protein

Since UAF1, a binding partner of USP1, has DNA-binding activity (Liang et al., 2016), we reasoned that USP1 might also stabilize replication forks through a DNA-binding mechanism. To test this hypothesis, we performed electrophoretic mobility shift assays with purified UAF1 protein with or without purified USP1 protein to analyze direct DNA-binding activity. Purified proteins were incubated with either ssDNA, dsDNA, or fork DNA and visualized by native polyacrylamide gel electrophoresis. The UAF1 protein and the USP1-UAF1 complex generated a gel shift of all three DNA templates. Interestingly, free USP1 also generated an upward shift of double-strand DNA and, more strongly, of fork DNA, indicating that USP1 alone can bind DNA (see arrows in Figure 3A, lane 11 and Figure 3B, lane 6).

USP1, USP12, and USP46 are related DUB proteins that bind to UAF1 and are stimulated by UAF1 (Cohn et al., 2007, 2009; Dahlberg and Juo, 2014; Li et al., 2016; Yin et al., 2015). All three proteins contain a conserved UAF1-binding site localized to a zinc-finger region of each polypeptide (Figure S3A). These USPs bind to a discrete WD40 domain of UAF1 (Li et al., 2016; Yin et al., 2015). Of the three proteins, USP1 is the largest protein, as shown by the sequence alignment with USP12 and USP46 (Figures S3A and S3B). While USP1 binds and shifts fork DNA upward (Figure 3C, lanes 1–6), USP12 fails to bind DNA (lanes 7–12), suggesting that the DNA-binding region of USP1 is localized to nonconserved regions of these two proteins.

By aligning the amino acid sequence of USP1 and USP12, we generated the cDNA encoding a truncated form of USP1 (USP1-Trunc) designed to eliminate regions of USP1 that are not conserved with USP12 (Figures 3D, S3A, and S3B). USP1-Trunc still contains the critical Cys, His, and Asp residues known to comprise the catalytic triad of the active ubiquitin protease (Eletr and Wilkinson, 2014). USP1-Trunc also contains the two critical amino acids (Cys 443 and Glu 514) required for binding and activation by UAF1 (Li et al., 2016; Yin et al., 2015). USP1-Trunc does not contain the autocleavage site previously identified in full-length USP1 (Huang et al., 2006). As predicted, USP1-Trunc failed to bind and gel shift the fork DNA structure (Figure 3D, lanes 8–12), confirming that the critical DNA-binding regions of USP1 exist within the deleted amino acid sequences.

To further localize a possible DNA-binding domain of USP1, we evaluated USP1 mutant proteins using a chromatin-binding assay (Figure 3E). Wild-type USP1 bound to chromatin; however, USP1-Trunc and USP1-Δ270-307 mutants had reduced binding to chromatin (Figure 3E). Region 2 of USP1 (from amino acids 270–307), also deleted in USP1-Trunc, was required for DNA binding, and positively charged lysine residues in this region may contribute to the DNA-binding activity. USP12 and USP46 are known to interact with both UAF1 and an additional WD40-containing protein, WDR20 (Kee et al., 2010; Sowa et al., 2009). USP1 is a larger protein than USP12 or USP46. Accordingly, USP1 may contain sequences that functionally substitute for WDR20 sequences in the assembled DUB multisubunit complex (see schematic, Figure S3C). Collectively, these results suggest that similar to UAF1, USP1 also exhibits a DNA-binding activity with enhanced binding to fork DNA structures.

The Deubiquitinating Activity of USP1 Is Stimulated by DNA Binding

Since USP1 is a deubiquitinase with DNA-binding activity, DNA may act as a cofactor altering its deubiquitinating activity. To test this possibility, we examined the ubiquitin protease activity of full-length USP1 bound in a complex with UAF1, with or without DNA, using the ubiquitin-7-amido-4-methylcoumarin (AMC) release assay and the ubiquitin CHOP2-Reporter assay (Figure 4A) (Cohn et al., 2007, 2009; Davis et al., 2016; Kee et al., 2010; Mistry et al., 2013). Interestingly, DNA stimulated a time-dependent increase in DUB activity of the USP1-UAF1 complex (Figure 4B). Maximal DUB stimulation was achieved with fork DNA, consistent with the stronger USP1-binding activity for this template. dsDNA also generated maximal DUB stimulation (Figure 4B). Fork DNA increased the DUB activity of the USP1-UAF1 complex at a 1:1 stoichiometry, with no further increase in DUB activity with additional DNA (Figure 4C).

In contrast to the USP1-UAF1 complex, DNA did not stimulate the activity of the USP12-UAF1-WDR20 complex, consistent with the lack of DNA-binding activity of USP12 (Figure 4D). UAF1 stimulated the DUB activity of USP1-Trunc, consistent with the presence of both the DUB catalytic triad and the UAF1 interaction domain of USP1-Trunc (Figures 3D, S3A, and S4A). Interestingly, DNA failed to stimulate the DUB activity of the USP1-Trunc-UAF1 complex (Figure 4E), indicating that DNA binding is required for DNA stimulated DUB activity. Since UAF1 has direct DNA-binding activity and the DNA-binding site of UAF1 remains unknown (Liang et al., 2016), it is unclear whether DNA binding to UAF1 also contributes to DUB activity stimulation. However, the lack of DNA stimulation of the USP1-Trunc-UAF1 complex suggests that the DNA binding of UAF1 alone is insufficient to stimulate USP1 DUB activity and that the direct binding of USP1 to DNA is required.

DNA Binding to USP1-UAF1 Enhances Ubiquitin Substrate Binding and Turnover

To gain further insight into the dynamics of USP1-UAF1 activation by DNA, we investigated the kinetics of complex activation. An *in vitro* enzymatic assay of the purified USP1-UAF1 complex, using Ub-AMC as a substrate, was established (Figures 4F and 4G). In order to determine the kinetic parameters of the USP1-UAF1 complex alone compared to the USP1-UAF1-fork DNA

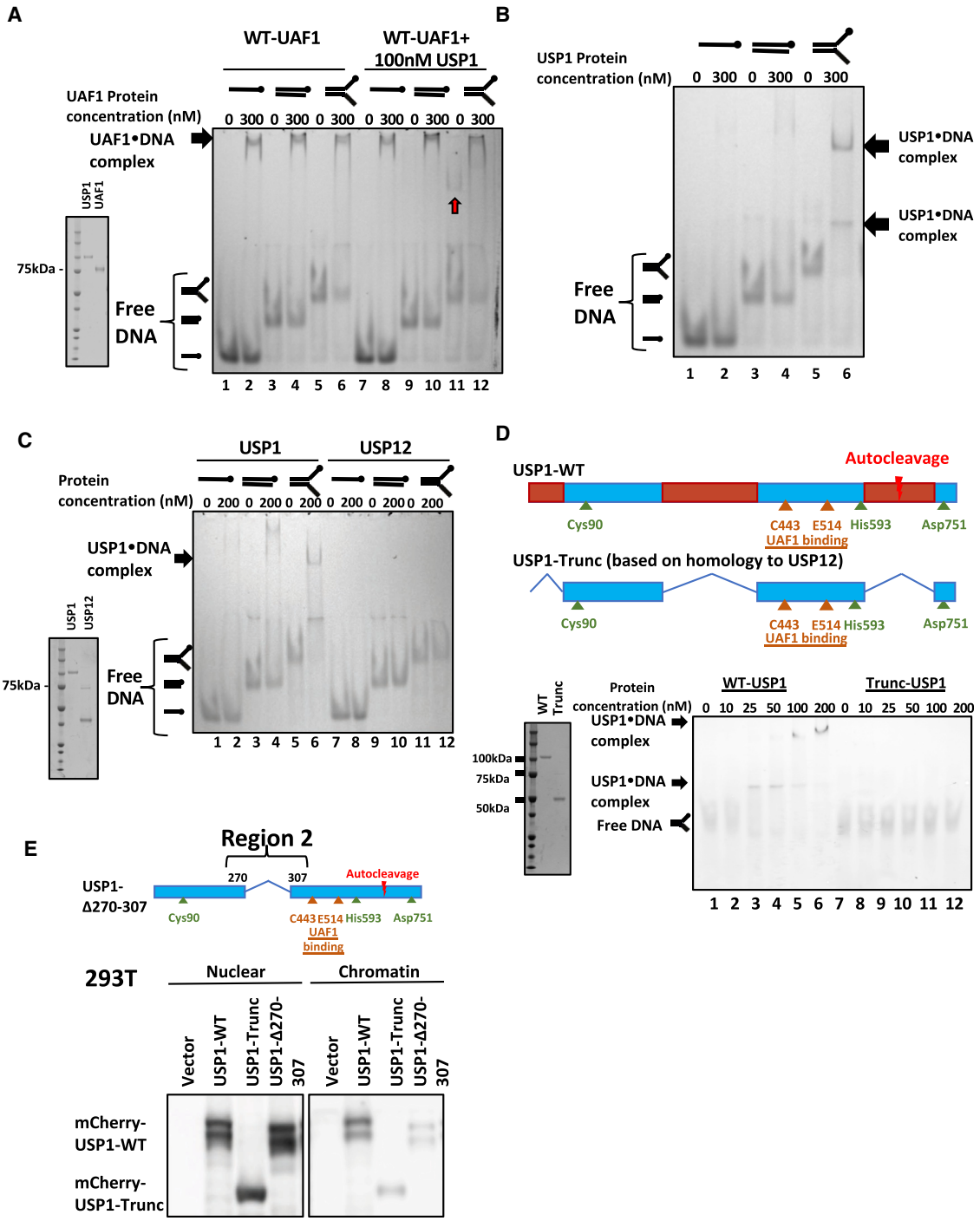

Figure 3. USP1 Is a DNA-Binding Deubiquitinase

(A) Coomassie blue stain of USP1 and UAF1 (left) showing purity of the proteins and electromobility shift gel showing DNA-binding activity of UAF1 and UAF1 + USP1 (right). Wild-type UAF1 or wild-type UAF1 + 100 nM USP1 proteins were incubated with ssDNA, dsDNA, or fork DNA, and electromobility shift of the DNA was analyzed. Note that a band in lane 11 (shown in red arrow) shows binding of USP1 alone to fork DNA.

(B) Electromobility shift gel showing a strong binding of USP1 to fork DNA. USP1 protein was incubated with ssDNA, dsDNA, or fork DNA, and electromobility shift of the DNA was analyzed.

(C) Coomassie blue stain of USP1 and USP12 showing purity of the proteins (left) and electromobility shift gel (right) showing absence of DNA-binding activity of USP12. USP1 and USP12 proteins were incubated with ssDNA, dsDNA, or fork DNA, and electromobility shift of the DNA was analyzed.

(legend continued on next page)

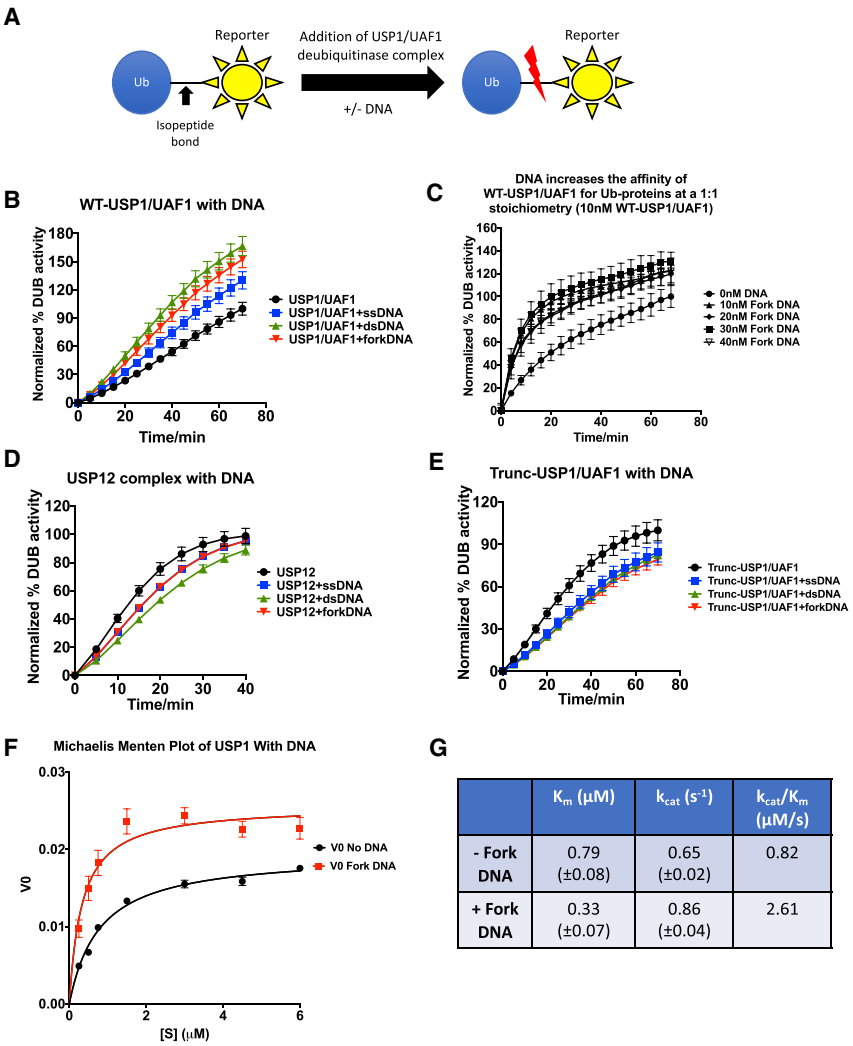

	K_m (μM)	k_{cat} (s^{-1})	k_{cat}/K_m (μM/s)
- Fork DNA	0.79 (±0.08)	0.65 (±0.02)	0.82
+ Fork DNA	0.33 (±0.07)	0.86 (±0.04)	2.61

Figure 4. DNA Stimulates the Deubiquitination Activity of the USP1/UAF1 Complex

(A) Schematic of ubiquitin reporter assays used.

(B) Ub-CHOP2-Reporter deubiquitination assay measuring wild-type USP1-UAF1 deubiquitinating activity with no DNA, ssDNA, dsDNA, and fork DNA. The deubiquitinating activity of wild-type USP1-UAF1 with no DNA is significantly less than that of wild-type USP1-UAF1 with ssDNA, dsDNA and fork DNA (n = 10).

(C) Ub-AMC enzymatic assay measuring wild-type USP1-UAF1 deubiquitination activity with increasing concentrations of fork DNA (n = 2).

(D) Ub-CHOP2-Reporter deubiquitination assay measuring wild-type USP12-UAF1-WDR20 (USP12 complex) deubiquitination activity with no DNA, ssDNA, dsDNA, and fork DNA (n = 2).

(E) Ub-CHOP2-Reporter deubiquitination assay measuring Trunc-USP1-UAF1 deubiquitination activity with no DNA, ssDNA, dsDNA, and fork DNA (n = 3).

(F and G) Michaelis-Menten plot of the deubiquitination activity of wild-type USP-UAF1 with fork DNA measured by the Ub-AMC enzymatic assay (F) and the K_M and k_{cat} values obtained from the Michaelis-Menten plot (G). Wild-type USP1 and wild-type UAF1 proteins were purchased from Boston Biochem, while the wild-type USP12-UAF1-WDR20 complex and Trunc-USP1 proteins were made in SF9 cells or *E. coli*.

Values in all the plots are mean ± SEM. See also Figure S4.

complex, the deubiquitination reaction was performed with a limiting amount of enzyme and an excess of substrate, and the initial velocity (V_0) was obtained. By measuring the substrate conversion at increasing substrate concentrations (Figure 4F), we determined that the affinity of the USP1-UAF1 complex for its ubiquitinated substrate is modestly influenced by DNA binding, decreasing the K_M from 0.79 μM to 0.33 μM (Figure 4G). Also, the catalytic turnover was modestly influenced by DNA binding, increasing the k_{cat} value 1.3-fold. As a result, the k_{cat}/K_M ratio is 3-fold higher for the USP1-UAF1-DNA complex compared to the USP1-UAF1 complex alone. Taken together, DNA regulates the deubiquitination activity of the USP1-UAF1 complex by increasing both substrate affinity and turnover.

A Specific Inhibitor of USP1, ML323, Inhibits the DUB Activity of USP1-Trunc but Does Not Inhibit DNA Binding

A specific inhibitor of USP1, ML323, was recently identified which blocks FANCD2 deubiquitination, causes an accumulation of cellular FANCD2-Ub and causes cellular hypersensitivity to cisplatin (Liang et al., 2014). Although ML323 binds directly to USP1, the binding site has not been determined. Interestingly, ML323 inhibits USP1-Trunc, as well as wild-type, full-length USP1, indicating that the ML323-binding sites are preserved in the USP1-Trunc protein (Figure S4B). Moreover, ML323 binding does not interfere with the DNA-binding activity of full-length USP1 (Figure S4C). Consistent with this result, ML323 also inhibits the DUB activity of the USP12-UAF1-WDR20 complex, which does not exhibit DNA binding activity (data not shown). Taken together, the inhibitory activity of ML323 does not result from the inhibition of DNA binding to USP1.

(D) Schematic representation of wild-type USP1 and Trunc-USP1 (top). Coomassie blue stain of wild-type USP1 and Trunc-USP1 (bottom left) and electromobility shift gel showing absence of DNA-binding activity of Trunc-USP1 (bottom right). Wild-type USP1 and Trunc-USP1 proteins were incubated with fork DNA, and electromobility shift of the DNA was analyzed (bottom right).

(E) Top: schematic representation of USP1-Δ270–307 mutant showing deletion in region 2 of USP1. Bottom: chromatin fractionation of the lysates from 293T cells transfected with vector, mCherry-USP1 wild-type, and mCherry-USP1-Trunc and mCherry-USP1-Δ270–307 showing reduced localization of USP1-Δ270–307 and USP1-Trunc to the chromatin.

See also Figure S3.

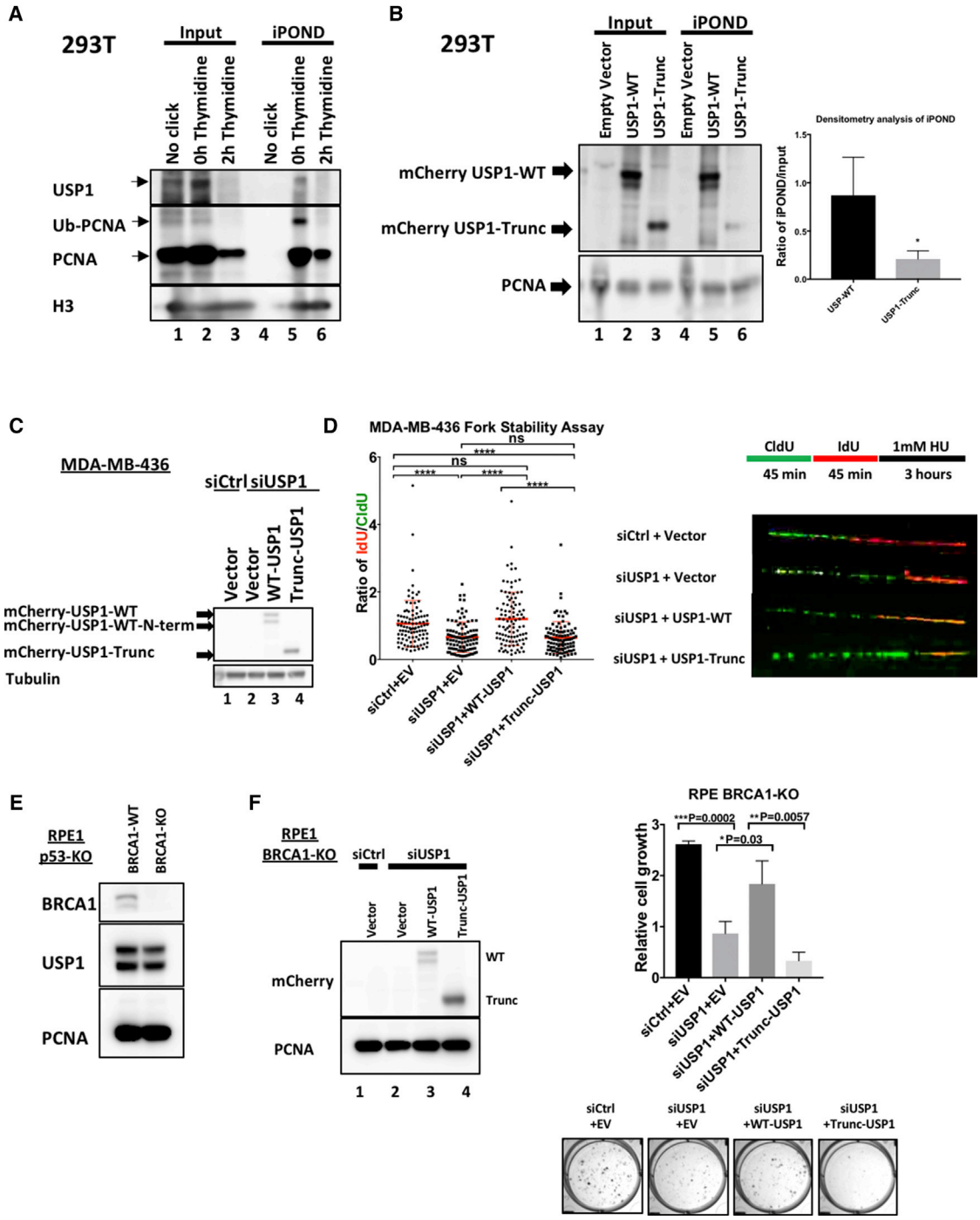

Figure 5. The DNA-Binding Activity of USP1 Is Required for Its Localization to the Replication Fork and for Stabilization of the Replication Fork

(A) iPOND blot with thymidine chase showing USP1 and PCNA decreasing at the replication fork following a 2-hr treatment with thymidine (n = 2).

(B) Left: iPOND blot of 293T cells transfected with vector control, mCherry-tagged wild-type USP1, or Trunc-USP1 and probed with antibody against mCherry and PCNA. Right: densitometry analysis of the iPOND blot (n = 3) (*p = 0.0475).

(C) Western blot of the lysates from BRCA1-deficient MDA-MB-436 cells treated with siCtrl or siUSP1 and rescued with empty vector, wild-type USP1, or USP1-Trunc.

(D) Left: graphical quantification of a DNA fiber experiment measuring hydroxyurea-mediated replication fork instability in BRCA1-deficient cells following treatment with siCtrl or siUSP1 and rescued with empty vector, wild-type USP1, or USP1-Trunc ($p < 0.0001$). Right: schematic of CldU, IdU, and hydroxyurea treatment (top), and representative images of the fibers from each treatment condition (bottom). The fiber assays were repeated twice with at least 100 fibers per

(legend continued on next page)

USP1-UAF1 DNA-Binding Activity Is Required for Localization of the DUB Complex to the Replication Fork

Recent studies suggest that the USP1-UAF1 complex might play a regulatory role at the advancing replication fork by controlling the local level of critical ubiquitinated substrates. Using a method of isolation of proteins on nascent DNA (iPOND) mass spectrometry, Dungrawala et al. (2015) identified USP1, UAF1 (WDR48), PCNA, and the FANCI-FANCD2 complex (ID complex) at sites of nascent DNA (Dungrawala et al., 2015). Interestingly, the USP1-UAF1 complex moves with the elongating replication fork, and fork stalling following hydroxyurea exposure displaces the complex. Another study, which compared the relative abundance of USPs on nascent and mature chromatin by iPOND, also demonstrated USP1 enrichment at the replisome (Lecona et al., 2016). These studies suggest that USP1 localizes at the replication fork and may contribute to replication fork protection by deubiquitinating co-localized critical substrates. Other studies demonstrate that replication stress causes USP1 autocleavage, suggesting a plausible mechanism for the regulated release of USP1-UAF1 from the fork (Huang et al., 2006).

We next confirmed that USP1 localizes to the replication fork using iPOND (Sirbu et al., 2011). Replication fork proteins were enriched by iPOND (Dungrawala and Cortez, 2015) and identified by immunoblotting (Figure 5A). As expected, similar to PCNA, USP1 was pulled down with nascent DNA and disappeared following thymidine chase, suggesting that USP1 localizes to the replication fork (Figure 5A). Since USP1-Trunc fails to bind DNA, we predicted that it would not localize to the replication fork. Using transient transfections of mCherry-USP1 wild-type or mCherry-USP1-Trunc in 293T cells, we performed an iPOND experiment followed by a western blot (Figure 5B). As predicted, wild-type USP1, but not USP1-Trunc, localized to the replication fork, indicating that DNA binding is required for USP1 fork localization (Figure 5B, left panel, lanes 5 and 6). PCNA localization was also found at the replication fork, as expected (Figure 5B). The USP1-Δ270-307 mutant with defective DNA-binding activity also showed reduced localization to the replication fork (Figure S5A).

DNA-Binding Activity of USP1 Is Required for Fork Protection and Cell Survival in BRCA1-Deficient Cells

Since the DNA-binding activity is required for localization of USP1 to the replication fork, we examined its role in fork protection in BRCA1-deficient cells. Knockdown of USP1 in BRCA1 deficient MDA-MB-436 breast cancer cells destabilized the replication fork after hydroxyurea blockade (Figures 5C and 5D). Complementation with wild-type USP1, but not the DNA-binding mutant USP1-Trunc, restored normal replication fork stability (Figures 5C, 5D, and S5B). USP1-Δ270–307 mutant also failed to rescue the replication fork instability in BRCA1-deficient cells following USP1 silencing (Figure S5C).

In order to confirm this finding in a null genetic background, we performed a CRISPR-Cas9-mediated knockout of BRCA1 in normal RPE cells. TP53 was first knocked out by CRISPR-Cas9, and a single-cell subclone was generated. Subsequently, BRCA1 was knocked out by CRISPR-Cas9, and a $p53^{-/-}$, $BRCA1^{-/-}$ RPE subclone was identified. This clone is both p53 and BRCA1 deficient, with no other known genetic aberrations (Figures 5E and S5D). The $p53^{-/-}$, $BRCA1^{-/-}$ RPE cells were highly sensitive to PARP inhibitor treatment, while $p53^{-/-}$, $BRCA1^{+/+}$ cells were resistant (Figure S5E).

Silencing of USP1 inhibited the growth of BRCA1-deficient RPE cells, as expected. Transfection with the wild-type USP1 cDNA, but not the Trunc-USP1 cDNA, rescued the growth defect, suggesting that the DNA-binding function of USP1 is required for the growth and survival of BRCA1-deficient RPE cells (Figure 5F). Similar results were obtained with BRCA1-deficient MDA-MB-436 cells (data not shown). U2OS cells with CRISPR-Cas9-mediated knockout of USP1 were also generated. As expected, these cells exhibited increased PCNA-Ub and FANCD2-Ub. Wild-type USP1, but not the USP1-Trunc, complemented these cells biochemically and functionally in a chromosomal break assay (Figures S5F and S5G).

Silencing of RAD18 and POLK Rescues the Synthetic Lethality between USP1 and BRCA1

USP1 expression correlates with PCNA expression in breast and ovarian carcinomas (Figures S6A and S6B). Since USP1 is a deubiquitinase with a known replication fork protein (PCNA-Ub) as its substrate (Huang et al., 2006), we reasoned that persistent monoubiquitination of this substrate following USP1 inhibition may contribute to the replication fork instability. We therefore performed iPOND following hydroxyurea treatment in 293T cells and assessed the recruitment of PCNA-Ub and USP1 at the stalled fork. Monoubiquitinated PCNA levels increased at the replication fork following hydroxyurea mediated fork stalling, corresponding to a decrease in local USP1 (Figures 6A, S6C, and S6D). As expected, PCNA-Ub levels increased after CRISPR-mediated knockout of USP1 or UAF1 in RPE-1 cells (Figures 6B and 6C). An increase in PCNA-Ub, corresponding to a decrease in USP1, was observed after hydroxyurea treatment (Figures 6A, S6C, and S6D). Taken together, these results suggest that the timely deubiquitination of PCNA by USP1 is critical for replication fork stability and that the aberrant accumulation of monoubiquitinated PCNA and its substrates might lead to fork instability. Indeed, silencing RAD18, the monoubiquitin ligase for PCNA, rescued the replication fork instability of BRCA1-deficient cells following USP1 inhibition (Figures 6D–6F and S6E).

condition, and the data from a representative experiment are shown. The median values for siCtrl + vector, siUSP1 + vector, siUSP1 + wild-type and siUSP1 + Trunc are 0.9434, 0.5907, 1.018, and 0.5801, respectively.

(E) Western blot of the lysates from p53-deficient RPE cells confirming the loss of BRCA1.

(F) Left: western blot of the lysates from BRCA1-deficient RPE cells treated with siCtrl or siUSP1 and rescued with empty vector, wild-type USP1, or USP1-Trunc. Right: graphical quantification (top) and representative images of colonies (bottom) after a clonogenic assay of BRCA1-deficient RPE cells transfected with siCtrl or siUSP1 and complemented with empty vector (EV), wild-type USP1, or Trunc-USP1 (n = 2).

See also Figure S5.

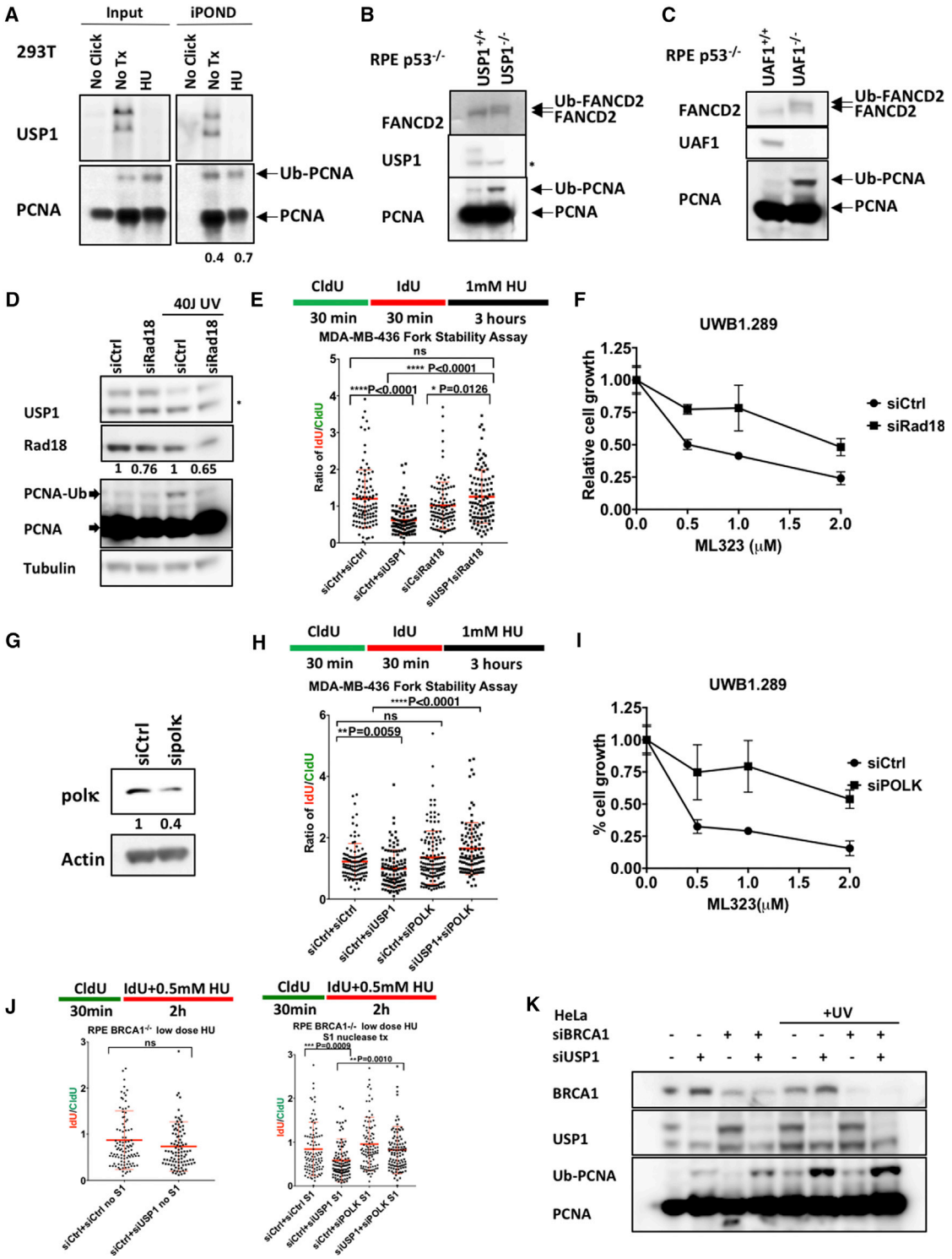

Figure 6. USP1-Mediated Replication Fork Instability in BRCA1-Deficient Cells Is Rescued by Inhibition of PCNA Monoubiquitination

(A) iPOND blot of 293T cells showing USP1 levels and Ub-PCNA levels following hydroxyurea treatment. The ratio of the long ubiquitinated form (L) versus the short un-ubiquitinated form (S) (L/S ratio) for PCNA is shown below the blot (n = 5).

(B) Western blot of the lysates from RPE p53$^{-/-}$ cells with CRISPR-mediated knockout of USP1.

(C) Western blot of the lysates from RPE p53$^{-/-}$ cells with CRISPR-mediated knockout of UAF1. Increased monoubiquitination of both FANCD2 and PCNA are seen in USP1$^{-/-}$ and UAF1$^{-/-}$ cells.

(legend continued on next page)

Aberrant recruitment of the DNA polymerase POLK, which is involved in TLS, has previously been shown to slow replication forks in a USP1-dependent manner (Jones et al., 2012). POLK expression is also significantly lower in BRCA1-mutated breast tumors than wild-type tumors (Figure S6F). Aberrant monoubiquitination of PCNA, leading to enhanced POLK recruitment, may therefore destabilize the replication fork in BRCA1-deficient cells. Indeed, silencing of POLK rescued the replication fork instability and viability of these cells following USP1 inhibition (Figures 6G–6I), thereby providing a mechanistic explanation for the toxicity resulting from USP1 knockdown. USP1 silencing resulted in increased POLK foci colocalization with BRCA1 foci (Figure S6G), suggesting that BRCA1 is required for fork stabilization in the setting of persistent POLK recruitment. Knockdown of REV1, another TLS polymerase recruited by PCNA-Ub, also resulted in replication fork protection (Figure S6H).

TLS polymerases exhibit low fidelity (Goodman and Woodgate, 2013). Persistent TLS polymerase recruitment may therefore cause replication fork destabilization through the introduction of aberrant replication products such as DNA gaps and mismatches. S1 nuclease is known to cleave DNA structures having gaps and mismatches (Vogt, 1973). S1 nuclease treatment specifically results in shorter DNA fibers due to the cleavage of the ssDNA gaps and mismatches and can be used for the detection of these gaps and mismatches (Quinet et al., 2016, 2017). In order to determine the presence of gaps and mismatches in the absence of USP1, we therefore performed a fiber assay along with S1 nuclease treatment. A low dose hydroxyurea (0.5 mM) treatment did not significantly affect the fork stability in BRCA1-deficient cells treated with siUSP1 (Figure 6J). However, S1 nuclease treatment resulted in shorter DNA fiber tracts resulting from cleavage of ssDNA gaps in BRCA1-deficient cells following USP1 knockdown (Figure 6J). Again, loss of the TLS polymerase POLK rescued this phenotype (Figure 6J). Taken together, the increased TLS activity after USP1 loss leads to increased ssDNA gaps in BRCA1-deficient cells.

Silencing of the nucleases DNA2 and MRE11 also rescued replication fork instability and viability in BRCA1-deficient cells following USP1 inhibition (Figures S6I and S7A). Reversed replication forks are degraded by MRE11 in BRCA1- or BRCA2-deficient cells (Kolinjivadi et al., 2017; Lemaçon et al., 2017; Mijic et al., 2017; Taglialatela et al., 2017; Vujanovic et al., 2017), and SMARCAL1 is known to promote fork reversal (Kolinjivadi et al., 2017). We reasoned that in the absence of USP1, SMARCAL1 contribute to fork reversal and enhanced fork degradation. Accordingly, SMARCAL1 knockdown rescued the fork degradation phenotype in BRCA1-deficient cells following USP1 loss (Figure S7B), suggesting that replication fork instability following USP1 depletion in BRCA1-deficient cells is dependent on fork reversal. In contrast, knockdown of the FAN1 nuclease did not rescue this phenotype (Figure S7C).

A recent study (Pathania et al., 2011) showed that UV strongly activates PCNA-Ub in BRCA1-deficient cells. We therefore assessed PCNA-Ub in HeLa cells after knocking down both USP1 and BRCA1. Loss of USP1 in BRCA1-deficient cells more strongly activated PCNA-Ub levels (Figure 6K). Taken together, the replication fork instability of cells deficient in BRCA1 and USP1 results from elevated levels of PCNA-Ub. Knockdown of RAD18, POLK, REV1, DNA2, MRE11, or SMARCAL1 rescues the replication fork instability in these cells.

Increased PCNA monoubiquitination results in the recruitment of POLK and other error-prone TLS polymerases (Choe and Moldovan, 2017). Accordingly, knockdown of USP1 in 293T cells resulted in the increased generation of point mutations as measured via the supF assay (Figure S7D) (Huang et al., 2006). Transfection with wild-type USP1, but not Trunc-USP1, reduced the mutagenesis level. Taken together, the toxicity resulting from increased PCNA monoubiquitination may be an indirect consequence of elevated TLS polymerase activity and TLS.

BRCA1-Deficient Cells with PARP Inhibitor Resistance Secondary to Fork Stabilization Are Sensitive to USP1 Inhibitors

PARP inhibitor resistance of BRCA1-deficient tumor cells can result from two major mechanisms: the restoration of HR repair and the stabilization of the replication fork (Bouwman et al.,

(D) Western blot of the lysates from UWB1.289 cells following Rad18 silencing. Values below the Rad18 blot indicate densitometry analysis of Rad18 protein levels.

(E) Schematic of CldU, IdU, and hydroxyurea treatment (top) and graphical quantification of a fiber assay measuring replication fork degradation in MDA-MB-436 cells following treatment with siCtrl, siUSP1, siRad18, or siUSP1 and siRad18 (bottom). The median values for siCtrl, siUSP1, siRad18, and siUSP1 + siRad18 are 0.9849, 0.5195, 0.8492, and 1.087, respectively. The fiber assays were repeated three times with at least 100 fibers quantified per condition, and the data from a representative experiment are shown.

(F) Dose-response curve of UWB1.289 cells following Rad18 silencing and treatment with the USP1 inhibitor ML323 (n = 3). Values represent mean ± SEM.

(G) Western blot of the lysates from UWB1.289 cells following POLK silencing. Values below the POLK blot indicate densitometry analysis of POLK protein levels.

(H) Schematic of CldU, IdU, and hydroxyurea treatment (top) and graphical quantification of a fiber assay in MDA-MB-436 cells following treatment with siCtrl, siUSP1, siPOLK, or siUSP1 and siPOLK (bottom). The median values for siCtrl, siUSP1, siPOLK, and siUSP1 + siPOLK are 1.1, 0.8663, 1.135, and 1.397, respectively. The fiber assays were repeated three times, and the data from a representative experiment are shown.

(I) Dose-response curve of UWB1.289 cells following POLK silencing and treatment with the USP1 inhibitor ML323 (n = 3). Values represent mean ± SEM.

(J) Fiber assays in BRCA1-deficient RPE cells treated with low-dose hydroxyurea (0.5 mM). Left: schematic of CldU, IdU, and hydroxyurea treatment (top) and graphical quantification of fibers from cells treated with siUSP1 and low-dose hydroxyurea (bottom). The median values for siCtrl and siUSP1 are 0.673 and 0.607, respectively. The fiber assay was performed once with at least 100 fibers quantified per condition. Right: schematic of CldU, IdU, and hydroxyurea treatment (top) and graphical quantification of fibers from cells treated with siUSP1 and low-dose hydroxyurea followed by S1 nuclease treatment. The median values for siCtrl, siUSP1, siPOLK, and siUSP1 + siPOLK are 0.664, 0.461, 0.808, and 0.753, respectively. The fiber assay was performed once with at least 100 fibers quantified per condition. Cells were treated with siRNAs and low-dose hydroxyurea followed by DNA extraction. DNA solutions were then treated with S1 nuclease before combing the DNA fibers onto coverslips.

(K) Western blot of the lysates from UV-treated HeLa cells with siRNA-mediated knockdown of USP1 and BRCA1.

See also Figures S6 and S7.

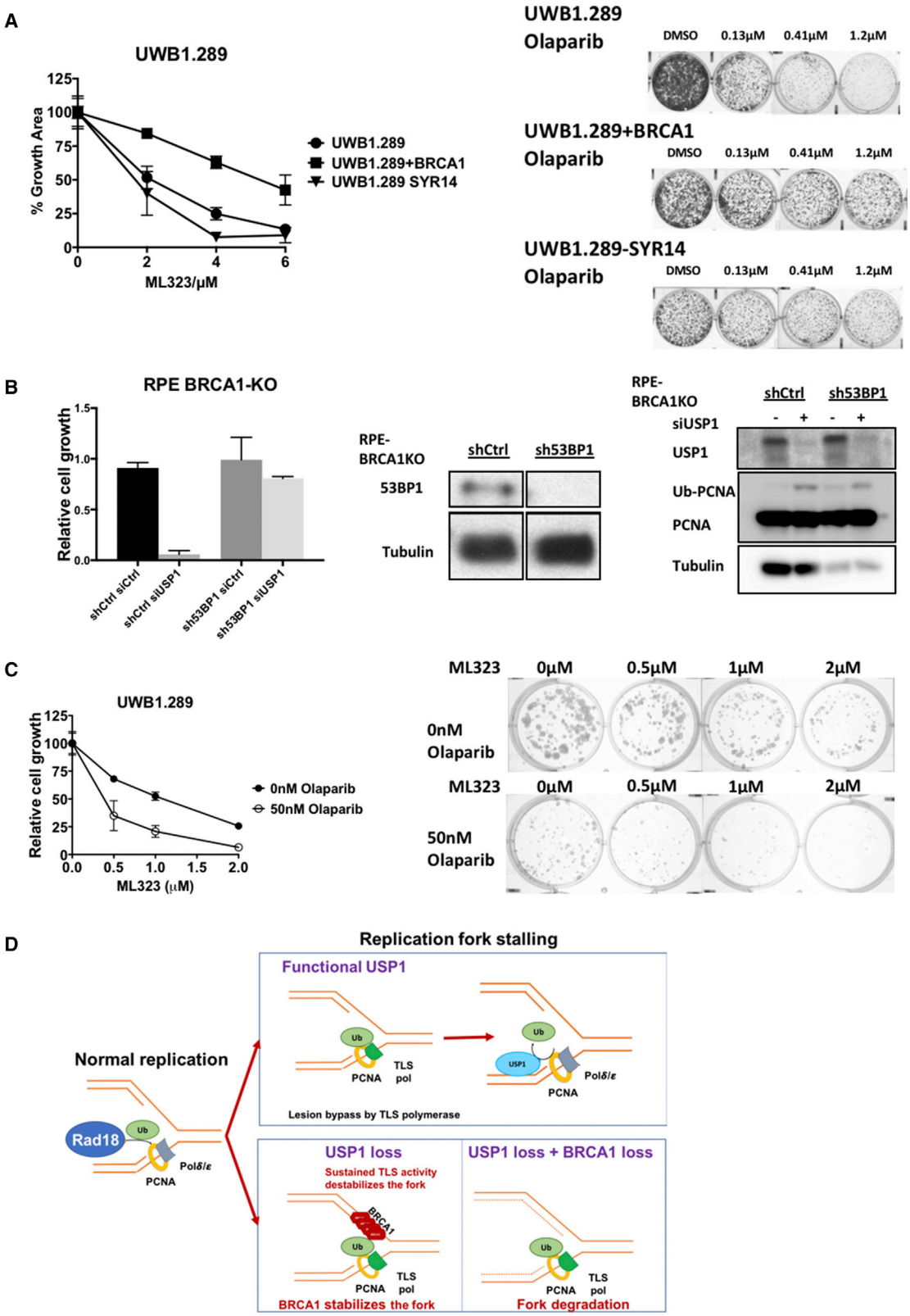

(legend on next page)

2010; Bunting et al., 2010; Ray Chaudhuri et al., 2016; Xu et al., 2015). BRCA1-deficient cells with acquired PARP inhibitor resistance resulting from these mechanisms have recently been generated (Yazinski et al., 2017). Interestingly, PARP-inhibitor-resistant cells resulting from fork stabilization remained sensitive to the USP1 inhibitor ML323 (Figure 7A). In contrast, PARP-inhibitor-resistant cells resulting from restoration of HR through 53BP1 silencing were resistant to the USP1 inhibitor (Figure 7B). Taken together, these results suggest that a subset of PARP-inhibitor-resistant BRCA1-deficient cells, including those that acquired resistance through fork stabilization, are sensitive to USP1 inhibition. Accordingly, USP1 inhibitors may be useful in the treatment of BRCA1-deficient tumors with acquired PARP inhibitor resistance through this mechanism.

Knockdown of USP1 in BRCA1-deficient cells results in increased PCNA monoubiquitination, increased fork resection, and subsequent cell death. Importantly, USP1 inhibitors may exhibit a monotherapy activity or potentiate the response of PARP inhibitors in BRCA1-deficient cells. Consistently, a USP1 inhibitor, ML323, enhanced the growth inhibition by a PARP inhibitor in BRCA1-deficient cells (Figure 7C). Collectively, our results support a model in which DNA-stimulated USP1 activity at the replication fork allows the survival of BRCA1-deficient cells. USP1 deubiquitinates PCNA-Ub at the replication fork and limits the toxic persistence of TLS activity (Figure 7D).

DISCUSSION

The USP1 substrates FANCD2-Ub and PCNA-Ub regulate replication fork events (Choe and Moldovan, 2017; Kais et al., 2016; Schlacher et al., 2012). FANCD2 is monoubiquitinated by the FA core E3 ligase complex, and PCNA is monoubiquitinated by RAD18. Both proteins are deubiquitinated by the USP1-UAF1 complex at the replication fork. FANCD2-Ub and PCNA-Ub can each recruit the nuclease FAN1 using the ubiquitin-binding pocket of FAN1, and FAN1 recruitment can prevent collapse of stalled forks (Lachaud et al., 2016; Porro et al., 2017). PCNA-Ub also recruits TLS polymerases, such as POLK and REV1, to the replication fork (Bi et al., 2006; Watanabe et al., 2004). Knockdown of USP1 in cell lines (Oestergaard et al., 2007) and a mouse model (Kim et al., 2009) results in upregulation of FANCD2-Ub and PCNA-Ub and DNA repair dysfunction. Whether USP1 knockdown also results in replication fork instability has not been previously evaluated. In the current study, we show that USP1 plays a critical role in protecting the replication fork in BRCA1-deficient cells by preventing the toxic PCNA-Ub-mediated recruitment of TLS polymerases to the fork. As a result, USP1 and BRCA1 are synthetic lethal.

Previous studies had suggested that the active USP1-UAF1 complex functions at the replication fork. For instance, USP1-UAF1 travels with the fork and is released from the fork upon hydroxyurea-mediated fork stalling (Dungrawala et al., 2015). This observation suggested that release of USP1-UAF1 might be an essential regulatory event controlling the hydroxyurea-mediated increase of FANCD2-Ub and PCNA-Ub. Moreover, the UAF1 subunit of the complex has a well-characterized DNA-binding function (Liang et al., 2016), further implying its possible function at the fork.

In the current study, we identify a DNA-binding property of USP1. We demonstrate that the USP1-UAF1 complex is localized to the replication fork and that its deubiquitinating activity is stimulated by a DNA structure mimicking a fork. Localization of the active enzyme to the fork is required for fork stabilization and reduction of PCNA-Ub levels at the fork. Interestingly, USP1-UAF1 is a unique DUB complex that is activated by DNA binding. Moreover, the most potent stimulant of its DUB activity is a DNA structure resembling a DNA replication fork. Recent studies indicate that DUB enzymes are often bound in complexes with allosteric binding partners. These structures offer an opportunity for the design of specific inhibitors that can disrupt allosteric activation of the complex (Li et al., 2016; Yin et al., 2015). Our results suggest that a small-molecule inhibitor of DNA binding to USP1-UAF1 might afford another avenue of DUB inhibitor development.

Our data also identify an important mechanism by which USP1 stabilizes the fork. Knockdown or small-molecule inhibition of USP1 activity results in the toxic accumulation of PCNA-Ub. Elevated PCNA-Ub results in elevated and persistent recruitment of the TLS polymerase POLK to the fork, leading to fork destabilization and increased single-base-pair mutagenesis. Consistent with these observations, the cellular toxicity resulting from elevated PCNA-Ub levels was reversed by the knockdown of the PCNA monoubiquitination ligase RAD18. A previous study has shown that PCNA ubiquitination is

Figure 7. PARP Inhibitor Augments the Growth Inhibition by USP1 Inhibitor in BRCA1-Deficient Cells

(A) Right: representative colony assays of UWB1.289 cells, UWB1.289+BRCA1 cells, and PARP-inhibitor-resistant UWB1.289-SYR14 cells treated with olaparib. Left: quantification of colonies after clonogenic assay of parental BRCA1-deficient UWB1.289 cells and PARP-inhibitor resistant UWB1.289 SYR14 cells treated with the USP1 inhibitor ML323 (n = 2). SYR14 cells were a kind gift from Dr. Lee Zou and have acquired PARP inhibitor resistance due to replication fork stabilization.

(B) BRCA1-deficient cells are known to restore HR capacity following the loss of 53BP1. Sensitivity of BRCA1-deficient RPE cells with small hairpin RNA (shRNA)-mediated knockdown of 53BP1 to USP1 depletion was determined. Quantitation of growth of BRCA1-deficient RPE cells with shRNA-mediated knockdown of 53BP1 followed by siRNA knockdown of USP1 is shown in the left panel (n = 2). Western blots of the lysates from BRCA1-deficient RPE cells with shRNA-mediated knockdown of 53BP1 followed by siRNA knockdown of USP1 are shown in the middle panel and right panel.

(C) Quantitation (left panel) and representative images of the colonies (right panel) after a clonogenic assay of BRCA1-deficient UWB1.289 cells exposed to graded concentrations of USP1 inhibitor ML323 in the presence or absence of the PARP inhibitor olaparib (n = 1). Values represent mean ± SEM.

(D) Schematic model of USP1-mediated fork stabilization. Upon replication fork stalling, RAD18-mediated monoubiquitination of PCNA facilitates switching of PCNA binding from replicative polymerases (polδ/ε) to TLS polymerases (e.g., POLK). Following lesion bypass by TLS polymerases, USP1 deubiquitinates PCNA, facilitating the conversion of PCNA binding back to replicative polymerases (polδ/ε). Loss of USP1 leads to replication fork destabilization due to persistent TLS polymerase loading and accumulation of toxic PCNA-Ub. BRCA1 is required to stabilize the replication fork. Therefore, loss of both USP1 and BRCA1 leads to replication fork degradation.

important, but not essential, for TLS in mammalian cells (Hendel et al., 2011).

In the absence of USP1, BRCA1 cellular phenotypes are exacerbated. While normal cells can tolerate the loss of USP1 and the elevated expression of toxic PCNA-Ub at the fork, BRCA1-deficient tumor cells cannot tolerate elevated PCNA-Ub levels. BRCA1-deficient cells already have fork instability, and the further knockdown of USP1 results in a synthetic lethal interaction. In the absence of USP1, a TLS polymerase, POLK, accumulates at the fork, leading to a reduction in replication fork speed (Jones et al., 2012). REV1, another TLS polymerase, also contributes to the fork instability in BRCA1-deficient cells. Taken together, our results suggest that BRCA1 plays a role in protecting the fork from excessive TLS. Previous studies have also investigated a role of BRCA1 in replication and TLS (Pathania et al., 2011; Tian et al., 2013; Urban et al., 2016). Consistent with our study, BRCA1-deficient cells accumulate PCNA-Ub at sites of replication in a RECQ5-helicase-dependent manner (Urban et al., 2016). In addition, a study by Pathania et al. (2011) also supports our findings, demonstrating that UV strongly activates PCNA-Ub in BRCA1-deficient cells. Indeed, we show that loss of USP1 in BRCA1-deficient cells more strongly activates PCNA-Ub. In contrast, another study (Tian et al., 2013) suggested that BRCA1 promotes ubiquitination of PCNA by regulating the recruitment of RAD18 to chromatin and directly recruits TLS polymerases (e.g., polymerase eta and REV1) to DNA damage sites.

Our data support a model in which elevated PCNA-Ub, but not elevated FANCD2-Ub (Kais et al., 2016), accounts for the synthetic lethality of BRCA1 and USP1. The FANCD2-Ub-mediated and PCNA-Ub-mediated recruitment of FAN1 to the replication fork does not appear to contribute to the observed fork-degradation phenotype in USP1-deficient cells. In contrast, the PCNA-Ub-mediated recruitment of TLS polymerases, such as POLK and REV1, destabilizes the fork in BRCA1 and USP1 double knockout cells through the introduction of DNA gaps and mismatches at the replication fork. Elevated fork reversal and nuclease digestion further destabilizes the fork, as a reduction in SMARCAL1, DNA2, and MRE11 expression is also protective.

Our results indicate that USP1 depletion is synthetic lethal with BRCA1 deficiency, but not with BRCA2 deficiency. Although both BRCA1 and BRCA2 protect replication forks from degradation, BRCA1 also has BRCA2-independent functions at stalled replication forks (Bunting et al., 2010; Pathania et al., 2011; Willis et al., 2017). For instance, BRCA1 deficiency leads to discrete chromosomal aberrations (namely, tandem duplications) at stalled forks (Nik-Zainal et al., 2016; Willis et al., 2017). The mechanisms that lead to fork protection in BRCA1- and BRCA2-deficient cells are also distinct. Destabilized forks are substrates for MUS81 nuclease-mediated remodeling only in BRCA2-deficient cells (Lemaçon et al., 2017; Rondinelli et al., 2017). Previous studies have shown that replication intermediates protected by either BRCA1 or BRCA2 contain reversed replication forks (Kolinjivadi et al., 2017; Lemaçon et al., 2017; Mijic et al., 2017; Taglialatela et al., 2017). These findings suggest that although BRCA1 and BRCA2 protect the same intermediates, their absence may activate alternative pathways of fork processing and restart. For instance, the fork processing and restart pathways are MUS81 dependent in the absence of BRCA2 and USP1 dependent in the absence of BRCA1, accounting for the synthetic lethality.

Importantly, the synthetic-lethal mechanism resulting from the combined knockdown of BRCA1 and USP1 has clinical implications. Multiple tumor types, including breast, ovarian, prostate, and pancreatic carcinomas, often have underlying defects in BRCA1 activity, resulting from germline or somatic mutations in the BRCA1 gene. These tumors, with underlying defects in HR repair and fork stability, are often sensitive to PARP inhibitors (Farmer et al., 2005). Since PARP inhibitor resistance is rapidly emerging in the clinic, through multiple independent mechanisms (Bouwman et al., 2010; Bunting et al., 2010; Jaspers et al., 2013; Ray Chaudhuri et al., 2016; Rondinelli et al., 2017; Xu et al., 2015), small-molecule inhibitors of USP1 may have clinical efficacy, as a monotherapy or in combination with PARP inhibitors, in BRCA1-deficient cancers. Tumor cells with acquired resistance to PARP inhibitors, resulting from replication fork stabilization, appear to be more vulnerable to USP1 inhibition than tumor cells with restored HR.

STAR★METHODS

Detailed methods are provided in the online version of this paper and include the following:

- KEY RESOURCES TABLE
- CONTACT FOR REAGENT AND RESOURCE SHARING
- EXPERIMENTAL MODEL AND SUBJECT DETAILS
  - Cell lines
  - Animal studies
- METHOD DETAILS
  - Generation of p53/BRCA1 knockout RPE-1 cells
  - Western blotting
  - iPOND
  - Replication combing assay
  - Sensitivity assays
  - Protein purification, *in vitro* deubiquitination assays and electromobility shift assays
  - Immunofluorescence
  - Cytogenetics
  - SupF mutagenesis assay
  - siRNA and sgRNA sequences
  - Quantitative real-time PCR
- QUANTIFICATION AND STATISTICAL ANALYSIS
  - Bioinformatics Analysis
  - USP1 dependency analysis
  - Statistical Analysis

SUPPLEMENTAL INFORMATION

Supplemental Information includes seven figures and can be found with this article online at https://doi.org/10.1016/j.molcel.2018.10.045.

ACKNOWLEDGMENTS

We thank all members of the D'Andrea laboratory for their helpful suggestions and comments. We also thank Alfredo Rodriguez for illustration of the model and Dr. Lee Zou for the kind gift of PARP-inhibitor-resistant UWB1.289

SYR14 cells. This research was supported by a Stand Up To Cancer (SU2C)-Ovarian Cancer Research Fund Alliance-National Ovarian Cancer Coalition Dream Team Translational Research Grant (SU2C-AACR-DT16-15). SU2C is a program of the Entertainment Industry Foundation. Research grants are administered by the American Association for Cancer Research, the scientific partner of SU2C. This work was also supported by the NIH (grants R37HL052725, P01HL048546, P50CA168504), the US Department of Defense (grants BM110181 and BC151331P1), as well as grants from the Breast Cancer Research Foundation and the Fanconi Anemia Research Fund (to A.D.D.) K.S.L. was supported by an A*STAR International Fellowship. N.Z. is an investigator of Howard Hughes Medical Institute.

AUTHOR CONTRIBUTIONS

K.S.L. conceived the study, performed experiments, analyzed data, and wrote the manuscript. H.L. designed the mutant USP1 under the supervision of N.Z. E.A.R. and E.F.G. performed *in vitro* deubiquitination assays. E.A.R. performed DNA fiber analyses and iPOND. C.C. created BRCA1-deficient RPE1 cells. K. Ponnienselvan performed supF assays. J.C.L. provided critical expertise on electromobility shift assays and *in vitro* deubiquitination assays under the guidance of T.Y. L.A.S. and C.Y. performed experiments. K. Parmar performed experiments and helped write the manuscript. D.K. helped with bioinformatics analysis. A.D.D. conceived the study and wrote the manuscript.

DECLARATION OF INTERESTS

The authors declare no competing interests.

Received: November 3, 2017
Revised: August 23, 2018
Accepted: October 29, 2018
Published: December 20, 2018

REFERENCES

Bi, X., Barkley, L.R., Slater, D.M., Tateishi, S., Yamaizumi, M., Ohmori, H., and Vaziri, C. (2006). Rad18 regulates DNA polymerase kappa and is required for recovery from S-phase checkpoint-mediated arrest. Mol. Cell. Biol. *26*, 3527–3540.

Bouwman, P., Aly, A., Escandell, J.M., Pieterse, M., Bartkova, J., van der Gulden, H., Hiddingh, S., Thanasoula, M., Kulkarni, A., Yang, Q., et al. (2010). 53BP1 loss rescues BRCA1 deficiency and is associated with triple-negative and BRCA-mutated breast cancers. Nat. Struct. Mol. Biol. *17*, 688–695.

Bunting, S.F., Callén, E., Wong, N., Chen, H.T., Polato, F., Gunn, A., Bothmer, A., Feldhahn, N., Fernandez-Capetillo, O., Cao, L., et al. (2010). 53BP1 inhibits homologous recombination in Brca1-deficient cells by blocking resection of DNA breaks. Cell *141*, 243–254.

Cancer Cell Line Encyclopedia Consortium; Genomics of Drug Sensitivity in Cancer Consortium (2015). Pharmacogenomic agreement between two cancer cell line data sets. Nature *528*, 84–87.

Cancer Genome Atlas Network (2012). Comprehensive molecular portraits of human breast tumours. Nature *490*, 61–70.

Cancer Genome Atlas Research Network (2011). Integrated genomic analyses of ovarian carcinoma. Nature *474*, 609–615.

Choe, K.N., and Moldovan, G.L. (2017). Forging ahead through darkness: PCNA, still the principal conductor at the replication fork. Mol. Cell *65*, 380–392.

Chu, W.K., Payne, M.J., Beli, P., Hanada, K., Choudhary, C., and Hickson, I.D. (2015). FBH1 influences DNA replication fork stability and homologous recombination through ubiquitylation of RAD51. Nat. Commun. *6*, 5931.

Cohn, M.A., Kowal, P., Yang, K., Haas, W., Huang, T.T., Gygi, S.P., and D'Andrea, A.D. (2007). A UAF1-containing multisubunit protein complex regulates the Fanconi anemia pathway. Mol. Cell *28*, 786–797.

Cohn, M.A., Kee, Y., Haas, W., Gygi, S.P., and D'Andrea, A.D. (2009). UAF1 is a subunit of multiple deubiquitinating enzyme complexes. J. Biol. Chem. *284*, 5343–5351.

Cukras, S., Lee, E., Palumbo, E., Benavidez, P., Moldovan, G.L., and Kee, Y. (2016). The USP1-UAF1 complex interacts with RAD51AP1 to promote homologous recombination repair. Cell Cycle *15*, 2636–2646.

D'Andrea, A., and Pellman, D. (1998). Deubiquitinating enzymes: a new class of biological regulators. Crit. Rev. Biochem. Mol. Biol. *33*, 337–352.

Dahlberg, C.L., and Juo, P. (2014). The WD40-repeat proteins WDR-20 and WDR-48 bind and activate the deubiquitinating enzyme USP-46 to promote the abundance of the glutamate receptor GLR-1 in the ventral nerve cord of Caenorhabditis elegans. J. Biol. Chem. *289*, 3444–3456.

Davis, M.I., and Simeonov, A. (2015). Ubiquitin-specific proteases as druggable targets. Drug Target Rev. *2*, 60–64.

Davis, M.I., Pragani, R., Fox, J.T., Shen, M., Parmar, K., Gaudiano, E.F., Liu, L., Tanega, C., McGee, L., Hall, M.D., et al. (2016). Small molecule inhibition of the ubiquitin-specific protease USP2 accelerates cyclin D1 degradation and leads to cell cycle arrest in colorectal cancer and mantle cell lymphoma models. J. Biol. Chem. *291*, 24628–24640.

Dungrawala, H., and Cortez, D. (2015). Purification of proteins on newly synthesized DNA using iPOND. Methods Mol. Biol. *1228*, 123–131.

Dungrawala, H., Rose, K.L., Bhat, K.P., Mohni, K.N., Glick, G.G., Couch, F.B., and Cortez, D. (2015). The replication checkpoint prevents two types of fork collapse without regulating replisome stability. Mol. Cell *59*, 998–1010.

Eletr, Z.M., and Wilkinson, K.D. (2014). Regulation of proteolysis by human deubiquitinating enzymes. Biochim. Biophys. Acta *1843*, 114–128.

Elia, A.E., Wang, D.C., Willis, N.A., Boardman, A.P., Hajdu, I., Adeyemi, R.O., Lowry, E., Gygi, S.P., Scully, R., and Elledge, S.J. (2015). RFWD3-dependent ubiquitination of RPA regulates repair at stalled replication forks. Mol. Cell *60*, 280–293.

Farmer, H., McCabe, N., Lord, C.J., Tutt, A.N., Johnson, D.A., Richardson, T.B., Santarosa, M., Dillon, K.J., Hickson, I., Knights, C., et al. (2005). Targeting the DNA repair defect in BRCA mutant cells as a therapeutic strategy. Nature *434*, 917–921.

Goodman, M.F., and Woodgate, R. (2013). Translesion DNA polymerases. Cold Spring Harb. Perspect. Biol. *5*, a010363.

Gudmundsdottir, K., and Ashworth, A. (2006). The roles of BRCA1 and BRCA2 and associated proteins in the maintenance of genomic stability. Oncogene *25*, 5864–5874.

Hendel, A., Krijger, P.H., Diamant, N., Goren, Z., Langerak, P., Kim, J., Reissner, T., Lee, K.Y., Geacintov, N.E., Carell, T., et al. (2011). PCNA ubiquitination is important, but not essential for translesion DNA synthesis in mammalian cells. PLoS Genet. *7*, e1002262.

Huang, T.T., Nijman, S.M., Mirchandani, K.D., Galardy, P.J., Cohn, M.A., Haas, W., Gygi, S.P., Ploegh, H.L., Bernards, R., and D'Andrea, A.D. (2006). Regulation of monoubiquitinated PCNA by DUB autocleavage. Nat. Cell Biol. *8*, 339–347.

Jaspers, J.E., Kersbergen, A., Boon, U., Sol, W., van Deemter, L., Zander, S.A., Drost, R., Wientjens, E., Ji, J., Aly, A., et al. (2013). Loss of 53BP1 causes PARP inhibitor resistance in Brca1-mutated mouse mammary tumors. Cancer Discov. *3*, 68–81.

Jones, M.J., Colnaghi, L., and Huang, T.T. (2012). Dysregulation of DNA polymerase κ recruitment to replication forks results in genomic instability. EMBO J. *31*, 908–918.

Kais, Z., Rondinelli, B., Holmes, A., O'Leary, C., Kozono, D., D'Andrea, A.D., and Ceccaldi, R. (2016). FANCD2 maintains fork stability in BRCA1/2-deficient tumors and promotes alternative end-joining DNA repair. Cell Rep. *15*, 2488–2499.

Kee, Y., Yang, K., Cohn, M.A., Haas, W., Gygi, S.P., and D'Andrea, A.D. (2010). WDR20 regulates activity of the USP12 x UAF1 deubiquitinating enzyme complex. J. Biol. Chem. *285*, 11252–11257.

Kim, J.M., Parmar, K., Huang, M., Weinstock, D.M., Ruit, C.A., Kutok, J.L., and D'Andrea, A.D. (2009). Inactivation of murine Usp1 results in genomic instability and a Fanconi anemia phenotype. Dev. Cell *16*, 314–320.

Kolinjivadi, A.M., Sannino, V., De Antoni, A., Zadorozhny, K., Kilkenny, M., Techer, H., Baldi, G., Shen, R., Ciccia, A., Pellegrini, L., et al. (2017). Smarcal1-mediated fork reversal triggers Mre11-dependent degradation of nascent DNA in the absence of Brca2 and stable Rad51 nucleofilaments. Mol. Cell *67*, 867–881.e867.

Komander, D., and Rape, M. (2012). The ubiquitin code. Annu. Rev. Biochem. *81*, 203–229.

Lachaud, C., Moreno, A., Marchesi, F., Toth, R., Blow, J.J., and Rouse, J. (2016). Ubiquitinated Fancd2 recruits Fan1 to stalled replication forks to prevent genome instability. Science *351*, 846–849.

Lecona, E., Rodriguez-Acebes, S., Specks, J., Lopez-Contreras, A.J., Ruppen, I., Murga, M., Muñoz, J., Mendez, J., and Fernandez-Capetillo, O. (2016). USP7 is a SUMO deubiquitinase essential for DNA replication. Nat. Struct. Mol. Biol. *23*, 270–277.

Ledermann, J., Harter, P., Gourley, C., Friedlander, M., Vergote, I., Rustin, G., Scott, C.L., Meier, W., Shapira-Frommer, R., Safra, T., et al. (2014). Olaparib maintenance therapy in patients with platinum-sensitive relapsed serous ovarian cancer: a preplanned retrospective analysis of outcomes by BRCA status in a randomised phase 2 trial. Lancet Oncol. *15*, 852–861.

Ledermann, J.A., Harter, P., Gourley, C., Friedlander, M., Vergote, I., Rustin, G., Scott, C., Meier, W., Shapira-Frommer, R., Safra, T., et al. (2016). Overall survival in patients with platinum-sensitive recurrent serous ovarian cancer receiving olaparib maintenance monotherapy: an updated analysis from a randomised, placebo-controlled, double-blind, phase 2 trial. Lancet Oncol. *17*, 1579–1589.

Lemaçon, D., Jackson, J., Quinet, A., Brickner, J.R., Li, S., Yazinski, S., You, Z., Ira, G., Zou, L., Mosammaparast, N., and Vindigni, A. (2017). MRE11 and EXO1 nucleases degrade reversed forks and elicit MUS81-dependent fork rescue in BRCA2-deficient cells. Nat. Commun. *8*, 860.

Leung, K.H., Abou El Hassan, M., and Bremner, R. (2013). A rapid and efficient method to purify proteins at replication forks under native conditions. Biotechniques *55*, 204–206.

Li, H., Lim, K.S., Kim, H., Hinds, T.R., Jo, U., Mao, H., Weller, C.E., Sun, J., Chatterjee, C., D'Andrea, A.D., and Zheng, N. (2016). Allosteric activation of ubiquitin-specific proteases by β-propeller proteins UAF1 and WDR20. Mol. Cell *63*, 249–260.

Liang, Q., Dexheimer, T.S., Zhang, P., Rosenthal, A.S., Villamil, M.A., You, C., Zhang, Q., Chen, J., Ott, C.A., Sun, H., et al. (2014). A selective USP1-UAF1 inhibitor links deubiquitination to DNA damage responses. Nat. Chem. Biol. *10*, 298–304.

Liang, F., Longerich, S., Miller, A.S., Tang, C., Buzovetsky, O., Xiong, Y., Maranon, D.G., Wiese, C., Kupfer, G.M., and Sung, P. (2016). Promotion of RAD51-mediated homologous DNA pairing by the RAD51AP1-UAF1 complex. Cell Rep. *15*, 2118–2126.

Lomonosov, M., Anand, S., Sangrithi, M., Davies, R., and Venkitaraman, A.R. (2003). Stabilization of stalled DNA replication forks by the BRCA2 breast cancer susceptibility protein. Genes Dev. *17*, 3017–3022.

Lord, C.J., and Ashworth, A. (2017). PARP inhibitors: Synthetic lethality in the clinic. Science *355*, 1152–1158.

Meyers, R.M., Bryan, J.G., McFarland, J.M., Weir, B.A., Sizemore, A.E., Xu, H., Dharia, N.V., Montgomery, P.G., Cowley, G.S., Pantel, S., et al. (2017). Computational correction of copy number effect improves specificity of CRISPR-Cas9 essentiality screens in cancer cells. Nat. Genet. *49*, 1779–1784.

Mijic, S., Zellweger, R., Chappidi, N., Berti, M., Jacobs, K., Mutreja, K., Ursich, S., Ray Chaudhuri, A., Nussenzweig, A., Janscak, P., and Lopes, M. (2017). Replication fork reversal triggers fork degradation in BRCA2-defective cells. Nat. Commun. *8*, 859.

Mistry, H., Hsieh, G., Buhrlage, S.J., Huang, M., Park, E., Cuny, G.D., Galinsky, I., Stone, R.M., Gray, N.S., D'Andrea, A.D., and Parmar, K. (2013). Small-molecule inhibitors of USP1 target ID1 degradation in leukemic cells. Mol. Cancer Ther. *12*, 2651–2662.

Moynahan, M.E., Chiu, J.W., Koller, B.H., and Jasin, M. (1999). Brca1 controls homology-directed DNA repair. Mol. Cell *4*, 511–518.

Moynahan, M.E., Pierce, A.J., and Jasin, M. (2001). BRCA2 is required for homology-directed repair of chromosomal breaks. Mol. Cell *7*, 263–272.

Nijman, S.M., Huang, T.T., Dirac, A.M., Brummelkamp, T.R., Kerkhoven, R.M., D'Andrea, A.D., and Bernards, R. (2005a). The deubiquitinating enzyme USP1 regulates the Fanconi anemia pathway. Mol. Cell *17*, 331–339.

Nijman, S.M., Luna-Vargas, M.P., Velds, A., Brummelkamp, T.R., Dirac, A.M., Sixma, T.K., and Bernards, R. (2005b). A genomic and functional inventory of deubiquitinating enzymes. Cell *123*, 773–786.

Nik-Zainal, S., Davies, H., Staaf, J., Ramakrishna, M., Glodzik, D., Zou, X., Martincorena, I., Alexandrov, L.B., Martin, S., Wedge, D.C., et al. (2016). Landscape of somatic mutations in 560 breast cancer whole-genome sequences. Nature *534*, 47–54.

Oestergaard, V.H., Langevin, F., Kuiken, H.J., Pace, P., Niedzwiedz, W., Simpson, L.J., Ohzeki, M., Takata, M., Sale, J.E., and Patel, K.J. (2007). Deubiquitination of FANCD2 is required for DNA crosslink repair. Mol. Cell *28*, 798–809.

Oza, A.M., Cibula, D., Benzaquen, A.O., Poole, C., Mathijssen, R.H., Sonke, G.S., Colombo, N., Špaček, J., Vuylsteke, P., Hirte, H., et al. (2015). Olaparib combined with chemotherapy for recurrent platinum-sensitive ovarian cancer: a randomised phase 2 trial. Lancet Oncol. *16*, 87–97.

Pathania, S., Nguyen, J., Hill, S.J., Scully, R., Adelmant, G.O., Marto, J.A., Feunteun, J., and Livingston, D.M. (2011). BRCA1 is required for postreplication repair after UV-induced DNA damage. Mol. Cell *44*, 235–251.

Pathania, S., Bade, S., Le Guillou, M., Burke, K., Reed, R., Bowman-Colin, C., Su, Y., Ting, D.T., Polyak, K., Richardson, A.L., et al. (2014). BRCA1 haploinsufficiency for replication stress suppression in primary cells. Nat. Commun. *5*, 5496.

Porro, A., Berti, M., Pizzolato, J., Bologna, S., Kaden, S., Saxer, A., Ma, Y., Nagasawa, K., Sartori, A.A., and Jiricny, J. (2017). FAN1 interaction with ubiquitylated PCNA alleviates replication stress and preserves genomic integrity independently of BRCA2. Nat. Commun. *8*, 1073.

Quinet, A., Martins, D.J., Vessoni, A.T., Biard, D., Sarasin, A., Stary, A., and Menck, C.F. (2016). Translesion synthesis mechanisms depend on the nature of DNA damage in UV-irradiated human cells. Nucleic Acids Res. *44*, 5717–5731.

Quinet, A., Carvajal-Maldonado, D., Lemacon, D., and Vindigni, A. (2017). DNA fiber analysis: mind the gap! Methods Enzymol. *591*, 55–82.

Ray Chaudhuri, A., Callen, E., Ding, X., Gogola, E., Duarte, A.A., Lee, J.E., Wong, N., Lafarga, V., Calvo, J.A., Panzarino, N.J., et al. (2016). Replication fork stability confers chemoresistance in BRCA-deficient cells. Nature *535*, 382–387.

Rondinelli, B., Gogola, E., Yücel, H., Duarte, A.A., van de Ven, M., van der Sluijs, R., Konstantinopoulos, P.A., Jonkers, J., Ceccaldi, R., Rottenberg, S., and D'Andrea, A.D. (2017). EZH2 promotes degradation of stalled replication forks by recruiting MUS81 through histone H3 trimethylation. Nat. Cell Biol. *19*, 1371–1378.

Schlacher, K., Christ, N., Siaud, N., Egashira, A., Wu, H., and Jasin, M. (2011). Double-strand break repair-independent role for BRCA2 in blocking stalled replication fork degradation by MRE11. Cell *145*, 529–542.

Schlacher, K., Wu, H., and Jasin, M. (2012). A distinct replication fork protection pathway connects Fanconi anemia tumor suppressors to RAD51-BRCA1/2. Cancer Cell *22*, 106–116.

Sirbu, B.M., Couch, F.B., Feigerle, J.T., Bhaskara, S., Hiebert, S.W., and Cortez, D. (2011). Analysis of protein dynamics at active, stalled, and collapsed replication forks. Genes Dev. *25*, 1320–1327.

Sowa, M.E., Bennett, E.J., Gygi, S.P., and Harper, J.W. (2009). Defining the human deubiquitinating enzyme interaction landscape. Cell *138*, 389–403.

Stephens, P.J., Tarpey, P.S., Davies, H., Van Loo, P., Greenman, C., Wedge, D.C., Nik-Zainal, S., Martin, S., Varela, I., Bignell, G.R., et al.; Oslo Breast

Cancer Consortium (OSBREAC) (2012). The landscape of cancer genes and mutational processes in breast cancer. Nature *486*, 400–404.

Taglialatela, A., Alvarez, S., Leuzzi, G., Sannino, V., Ranjha, L., Huang, J.W., Madubata, C., Anand, R., Levy, B., Rabadan, R., et al. (2017). Restoration of replication fork stability in BRCA1- and BRCA2-deficient cells by inactivation of SNF2-family fork remodelers. Mol. Cell *68*, 414–430.e418.

Thorslund, T., McIlwraith, M.J., Compton, S.A., Lekomtsev, S., Petronczki, M., Griffith, J.D., and West, S.C. (2010). The breast cancer tumor suppressor BRCA2 promotes the specific targeting of RAD51 to single-stranded DNA. Nat. Struct. Mol. Biol. *17*, 1263–1265.

Tian, F., Sharma, S., Zou, J., Lin, S.Y., Wang, B., Rezvani, K., Wang, H., Parvin, J.D., Ludwig, T., Canman, C.E., and Zhang, D. (2013). BRCA1 promotes the ubiquitination of PCNA and recruitment of translesion polymerases in response to replication blockade. Proc. Natl. Acad. Sci. USA *110*, 13558–13563.

Urban, V., Dobrovolna, J., Hühn, D., Fryzelkova, J., Bartek, J., and Janscak, P. (2016). RECQ5 helicase promotes resolution of conflicts between replication and transcription in human cells. J. Cell Biol. *214*, 401–415.

Villamil, M.A., Liang, Q., and Zhuang, Z. (2013). The WD40-repeat protein-containing deubiquitinase complex: catalysis, regulation, and potential for therapeutic intervention. Cell Biochem. Biophys. *67*, 111–126.

Vogt, V.M. (1973). Purification and further properties of single-strand-specific nuclease from Aspergillus oryzae. Eur. J. Biochem. *33*, 192–200.

Vujanovic, M., Krietsch, J., Raso, M.C., Terraneo, N., Zellweger, R., Schmid, J.A., Taglialatela, A., Huang, J.W., Holland, C.L., Zwicky, K., et al. (2017). Replication fork slowing and reversal upon DNA damage require PCNA polyubiquitination and ZRANB3 DNA translocase activity. Mol. Cell *67*, 882–890.e885.

Watanabe, K., Tateishi, S., Kawasuji, M., Tsurimoto, T., Inoue, H., and Yamaizumi, M. (2004). Rad18 guides poleta to replication stalling sites through physical interaction and PCNA monoubiquitination. EMBO J. *23*, 3886–3896.

Willis, N.A., Frock, R.L., Menghi, F., Duffey, E.E., Panday, A., Camacho, V., Hasty, E.P., Liu, E.T., Alt, F.W., and Scully, R. (2017). Mechanism of tandem duplication formation in BRCA1-mutant cells. Nature *551*, 590–595.

Xu, G., Chapman, J.R., Brandsma, I., Yuan, J., Mistrik, M., Bouwman, P., Bartkova, J., Gogola, E., Warmerdam, D., Barazas, M., et al. (2015). REV7 counteracts DNA double-strand break resection and affects PARP inhibition. Nature *521*, 541–544.

Yazinski, S.A., Comaills, V., Buisson, R., Genois, M.M., Nguyen, H.D., Ho, C.K., Todorova Kwan, T., Morris, R., Lauffer, S., Nussenzweig, A., et al. (2017). ATR inhibition disrupts rewired homologous recombination and fork protection pathways in PARP inhibitor-resistant BRCA-deficient cancer cells. Genes Dev. *31*, 318–332.

Ye, Y., Scheel, H., Hofmann, K., and Komander, D. (2009). Dissection of USP catalytic domains reveals five common insertion points. Mol. Biosyst. *5*, 1797–1808.

Yin, J., Schoeffler, A.J., Wickliffe, K., Newton, K., Starovasnik, M.A., Dueber, E.C., and Harris, S.F. (2015). Structural insights into WD-repeat 48 activation of ubiquitin-specific protease 46. Structure *23*, 2043–2054.

Yun, M.H., and Hiom, K. (2009). CtIP-BRCA1 modulates the choice of DNA double-strand-break repair pathway throughout the cell cycle. Nature *459*, 460–463.

Yusufzai, T., Kong, X., Yokomori, K., and Kadonaga, J.T. (2009). The annealing helicase HARP is recruited to DNA repair sites via an interaction with RPA. Genes Dev. *23*, 2400–2404.

STAR★METHODS

KEY RESOURCES TABLE

REAGENT or RESOURCE	SOURCE	IDENTIFIER
Antibodies		
FANCD2	Santa Cruz	F17; RRID:AB_2278211
USP1	Huang et al., 2006; Millipore; Bethyl	ABC413; A301-699A; RRID:AB_1211376
POLK	Bethyl	A301-975A; RRID:AB_1548018
RAD18	Novus	3H7; RRID:AB_547545
PCNA	Santa Cruz	PC-10; RRID:AB_628110
mCherry	Abcam	ab167453; RRID:AB_2571870
Tubulin	Abcam	ab6160; RRID:AB_305328
53BP1	Cell Signaling	4937; RRID:AB_10694558
Fan1	Invitrogen	PA525171; RRID:AB_2542671
MRE11	Novus Biologicals	NB100-142; RRID:AB_10077796
BRCA1	EMD Millipore	MS110; 07-434; RRID:AB_213438
SMARCAL1	(Yusufzai et al., 2009)	
Recombinant Proteins		
USP1	R&D Systems	E564
USP1/UAF1	R&D Systems	E568
Critical Commercial Assays		
Ub-Chop2 Reporter System	LifeSensors	PR1101
Experimental Models: Cell Lines		
293T	ATCC	CRL-3216
HeLa	ATCC	CCL-2
RPE1	ATCC	CRL-4000
UWB1.289	ATCC	CRL-2945
UWB1.289+BRCA1	ATCC	CRL-2946
UWB1.289-SYR14	Yazinski et al., 2017	Lee Zou's laboratory, Massachusetts General Hospital
Experimental Models: Organisms/Strains		
Athymic nude mice/Crl:NU(NCr)-Foxn1^{nu}	Charles River Laboratories	Strain code 490

CONTACT FOR REAGENT AND RESOURCE SHARING

Further information and requests for resources and reagents should be directed to and will be fulfilled by the Lead Contact, Alan D'Andrea (alan_dandrea@dfci.harvard.edu).

EXPERIMENTAL MODEL AND SUBJECT DETAILS

Cell lines

HeLa and 293T cells were purchased from ATCC and grown in DMEM (GIBCO) supplemented with 10% fetal bovine serum. MDA-MB-436 and MDA-MB-436+BRCA1 cells were a kind gift from Dr. Geoffrey Shapiro (Dana Farber Cancer Institute) and grown in RPMI (GIBCO) supplemented with 10% fetal bovine serum. RPE1 cells were purchased from ATCC and grown in DMEM/F12 (GIBCO) supplemented with 10% fetal bovine serum. UWB1.289, UWB1.289+BRCA1 cells were purchased from ATCC (Yazinski et al., 2017) and grown in RPMI (ATCC) and MEGM (Lonza) at a 1:1 ratio, supplemented with 3% fetal bovine serum. UWB1.289 SYR14 cells (Yazinski et al., 2017) were obtained from Dr. Lee Zou and were also grown in RPMI (ATCC) and MEGM (Lonza) at a 1:1 ratio, supplemented with 3% fetal bovine serum. All cell lines were cultured at 37°C in a humidified incubator.

Animal studies

Xenograft studies were approved by The Dana-Farber Cancer Institute's Animal Care and Use Committee. Five weeks old female athymic nude mice were purchased from Charles River laboratories and acclimatized at the animal facility of Dana-Farber Cancer Institute for four weeks. 2×10^6 breast cancer cells were then mixed with matrigel (BD Biosciences) and subcutaneously implanted into both flanks of mice. The tumor growth was monitored by caliper measurements (twice a week) and tumor volumes were calculated using a formula (length × width^2)/2.

METHOD DETAILS

Generation of p53/BRCA1 knockout RPE-1 cells

Oligonucleotides encoding guide RNAs targeting TP53 and BRCA1 were cloned into the pSpCas9(BB)-2A-GFP vector, a gift from Feng Zhang (Addgene plasmid # 48138). The targeted genomic sequences were GATCCACTCACAGTTTCCAT and TCTTGTGCT GACTTACCAGA for TP53 and BRCA1, respectively. The targeted genomic sequences for USP1 and UAF1 were CTTTCACTAGG TATGACACC and ACCGGCAGAACACAGCAGGG, respectively. RPE-1 cells were transfected with the CRISPR-Cas9 targeting construct to TP53 using Lipofectamine 2000 (Invitrogen, Cat #11668). 48 hours following transfection, GFP+ cells were selected and single cells were seeded using a BD FACSAria II cell sorter. Single cells were grown for approximately 3 weeks. TP53 knockout clones were identified by western blotting. The same procedure was used to knock out BRCA1 in a TP53 knockout RPE-1 cell line. BRCA1 knockout clones were identified by western blotting and confirmed by Sanger sequencing.

Western blotting

Cells were lysed with lysis buffer (300mM NaCl, 50mM Tris-Cl, 1mM EDTA, 0.5% NP-40), lysates were resolved on denaturing Nupage (Invitrogen) polyacrylamide gels and transferred onto nitrocellulose membranes. Membranes were blocked with 5% milk in TBST, and probed with primary and secondary antibodies respectively, then detected with chemiluminescence (Western Lightning, Perkin Elmer).

iPOND

Accelerated native iPOND was performed as described (Leung et al., 2013; Rondinelli et al., 2017). Briefly, 2-4 15cm dishes of 293T cells were plated at a density of 15 million cells per plate. Cells were pulsed with EdU for 10 min then treated with thymidine for 2 hours or hydroxyurea for 3 hours (Dungrawala and Cortez, 2015). Nuclei were then harvested and resuspended in click reaction mix containing biotin azide for an hour. Samples were next lysed and sonicated and streptavidin pull-down performed overnight at 4°C. Beads were washed 5-7 times then boiled with loading buffer containing 2-mercaptoethanol for 20 min. Samples were then resolved in Nupage (Invitrogen) polyacrylamide gels and transferred onto nitrocellulose membranes for blotting.

Replication combing assay

Replication combing assay was performed using the FiberComb machine (Genomic Vision). Briefly, cells were treated with CldU, IdU, then HU, with 3 PBS washes between each treatment. Treatment times are indicated in each figure. Cells were then trypsinized, counted and embedded in low melting point agarose plugs, then treated with proteinase k overnight. Agarose plugs were then washed and digested with agarase. Agarase-treated samples were then poured into FiberComb wells and combed onto silanized coverslips. Coverslips were probed with rat anti-BrdU antibody (clone BU1/75 (ICR1) specific to CldU, Life Technologies MA182088) and mouse anti-BrdU Antibody (specific to IdU, BD Biosciences 347580) and visualized by fluorescence microscopy. Pictures were taken of at least 100 fibers per condition. DNA fibers were measured with ImageJ and graphed. Each experiment was repeated at least three times unless otherwise stated. For S1 nuclease treatment, S1 nuclease (ThermoFisher Scientific) was added to DNA solution following agarase treatment and incubated at room temperature for 30 min. Nuclease treated samples were then poured into FiberComb wells and combed onto silanized coverslips.

Sensitivity assays

Cells were transfected with siRNA or plasmid 18-24h before being plated for colony formation assays. Cells were counted and plated in triplicates in 6-well plates. For treatment with USP1 inhibitor ML323 (Selleckchem, Texas, USA), plated cells were allowed to adhere overnight before treatment with ML323 the next day. At the end of the experiment, cells were fixed with methanol for 10 min at −20°C then stained with crystal violet. Plates were imaged with ImageQuant Las4000 (GE Healthcare) and quantification of cell growth area was performed with ImageJ.

Protein purification, *in vitro* deubiquitination assays and electromobility shift assays

Recombinant USP1 and UAF1 wild-type and mutant proteins were prepared in SF9 cells as previously described (Cohn et al., 2007). Recombinant USP1 and UAF1 proteins from R&D systems (E564, E566) were used for some electromobility shift assays and *in vitro* deubiquitination assays. Ub-CHOP2-Reporter assays (Life Sensors, PR1101) were performed according to manufacturer's instructions provided with the kit (Davis et al., 2016). Ub-AMC (R&D systems) assays were performed as previously described (Cohn et al., 2009; Cohn et al., 2007; Kee et al., 2010; Mistry et al., 2013). USP1/UAF1 enzyme was diluted in buffer (containing 0.1mg/ml

ovalbumin, 10mM DTT, 20mM pH7.8 HEPES, 20mM NaCl and 0.5mM EDTA) to a final concentration of 10nM. Single-stranded, double-stranded, fork DNA or an equivalent amount of water is added to the mix to a final concentration of 20nM. Samples were added to a 384-well black bottom plate (Westnet). Ub-AMC substrate was pipetted in just before plates were read. For k_{cat}/K_M calculations, a graph of Ub-AMC fluorescence-to-substrate conversion was first plotted by measuring fluorescence with known substrate concentrations. An excess of Ub-AMC substrate was added to known amounts of USP1/UAF1 enzyme. Initial velocity (V_o) was obtained by graphing time against substrate concentration and obtaining the slope from the first three time points (180 s) of each graph. Graphpad Prism was used to calculate k_{cat}, K_M and k_{cat}/K_M from V_o and enzyme concentrations. Electromobility shift assays were performed by pre-incubating fluorophore (Cy3)-tagged DNA and purified protein in binding buffer (20mM HEPES (pH 7.6), 0.1M KCl, 5mM MgCl2, 3% (v/v) glycerol, 0.25mg/ml BSA, 0.05mM EDTA, 0.5mM DTT, 0.01% (v/v) NP-40) for 30 min on ice. Samples were then loaded onto 6% polyacrylamide gels and ran at 65V in 0.5X TBE for 135min at 4°C. Gels were visualized using the LAS-4000 imaging system (GE Healthcare Life Sciences). DNAs used for Ub-AMC, Ub-CHOP2 and electromobility shift assay were 40bp in length and were designed to have minimal potential of secondary structure formation. The sequences were as follows: 40-mer top (5′-CCAGTGAATTGTTGCTCGGTACCTGCTAACGGTAATCGG-3′); 40-mer ds-bottom (5′-CCGATTACCGTTAGCAGGTACC GAGCAACAATTCACTGG-3′); 40-mer fork bottom (5′-CAGCTATGGGACATTCGATACCGAGCAACAATTCACTGG-3′). The K_M and k_{cat} values of USP1 were determined using the Ub-AMC assay as described previously (Cohn et al., 2007).

Immunofluorescence

Cells plated on coverslips were washed once with PBS and fixed with 4% paraformaldehyde for 10 minutes on ice. 0.5% Triton X-100 was added to cells for 30min for extraction. Coverslips were then blocked with 3% BSA for 30min and primary antibody to BRCA1 (Millipore #07-434) added (diluted 1:1000 in 3% BSA) overnight. Following overnight incubation, coverslips were washed three times with PBS, then anti-rabbit secondary antibody (Alexa Fluor, Life Technologies) added for 30min. Coverslips were then mounted with DAPI and visualized under the fluorescence microscope.

Cytogenetics

Cells were transfected with siRNAs twice for 48 hours and incubated for 48 hours in the presence or absence of 20ng/ml of MMC. Cells were exposed for 2 hours to colcemid (0.1ug/ml) and harvested using a 0.075M KCL hypotonic solution and fixed with 3:1 methanol: acetic acid. Slides were stained with Wright's stain and when possible, 50 metaphase spreads were scored for aberrations. Metaphase spreads were observed using a Zeiss Axio Imager microscope and captured using CytoVision software from Applied Imaging.

SupF mutagenesis assay

293T cells were transfected with the respective siRNA and plasmids and cultured for 48h. Next, the supF plasmid (pSP189) was damaged with 1000J/ cm^2 of UVC and transfected into the cells. After another 48h, the supF plasmid was extracted using a miniprep kit (Wizard plus SV miniprep kit, Promega). The unreplicated DNA was digested using DPN1 and the remaining pSP189 plasmid was ethanol precipitated and transformed into electrocompetent MBM7070, a strain of E.coli which has a mutated β galactosidase gene. The cells were then plated on agar plates containing 100 μg/ml ampicillin, 100 μg/ml of X-gal and 1 mM of IPTG. The number of white and blue colonies were counted and the mutation frequency was calculated by dividing the total number of white colonies by the total number white and blue colonies.

siRNA and sgRNA sequences

siRNA sequences against USP1 were 5′-TCGGCAATACTTGCTATCTTA-3′ and 5′- CCATACAAACATTGGTAAA-3′ (siRNA against 3′UTR) respectively. sgRNA sequence against USP1 and UAF1 were as follows:

USP1-F: CACCGGTCATACCTAGTGAAAGTAA
USP1-R: AAACTTACTTTCACTAGGTATGACC
UAF1-F: CACCGAGTGTCAACATGCAAGATGG
UAF1-R: AAACCCATCTTGCATGTTGACACTC

Other siRNA sequences were as follows:

POLK: 5′-AACCTCTAGAAATGTCTCATA-3′
Rad18: 5′-AAACTCAGTGTCCAACTTGCT-3′
SMARCAL1: 5′-AGAGCACAGUAAACUAAUUGCAAAG-3′
Rev1: 5′- CAGCGCATCTGTGCCAAAGAA-3′
Fan1: 5′- GCAGGAAGGCAGAGTGGCT-3′
DNA2: 5′- CAGTATCTCCTCTAGCTAGTT-3′
MRE11: 5′-GGGTTATTTGAGCAAGTAATT-3′

Quantitative real-time PCR

RNA was extracted using RNeasy Mini Kit (QIAGEN) and reverse transcribed with the SuperScriptIII kit (Thermo Fisher Scientific). Real-time PCR was performed with SYBR Green PCR Master Mix (Life Technologies). Primer sequences are as follows:

Rev1-F: GATGGAGGAAGCGAGCTGAAA
Rev1-R: CCTTCTGCATAGCAGCATCTG
GAPDH-F: TCATTTCCTGGTATGACAACG
GAPDH-R: TTACTCCTTGGAGGCCATGT

QUANTIFICATION AND STATISTICAL ANALYSIS

Bioinformatics Analysis

The Cancer Genome Atlas (TCGA) datasets were accessed through the public portal (http://www.cbioportal.org). Published TCGA datasets for breast and ovarian cancers were used in which both mutations and expression analyses were available (Cancer Genome Atlas Research Network, 2011; Stephens et al., 2012). USP1 expression in BRCA1 mutant tumors was compared against BRCA1 wild-type tumors. GraphPad Prism was used to graph the data and carry out statistical analyses (Student's t test). USP1 overexpression in basal-like breast cancers was confirmed using a separate dataset from the Gene Expression Omnibus (GEO: GDS2250).

USP1 dependency analysis

To assess USP1 dependency in breast and ovarian cancer cell lines by BRCA1 and BRCA2 mutation status, data extracted from the Broad Institute Cancer Dependency Map Achilles CRISPR Avana 17Q2 dataset (Meyers et al., 2017) and the Cancer Cell Line Encyclopedia (Cancer Cell Line Encyclopedia Consortium and Genomics of Drug Sensitivity in Cancer Consortium, 2015) were used. All 57 breast and ovarian cancer cell lines for which there were data on gene-knockout effects inferred by CERES (Meyers et al., 2017) and BRCA1 and BRCA2 mutation status were included in the analysis. Cell lines were grouped by presence or absence of a nonsynonymous BRCA1 or BRCA2 mutation. CERES gene dependency scores for USP1 in wild-type versus mutant groups were plotted using GraphPad Prism 7.03 (bars reflect mean ± SEM) and compared via the non-parametric Mann-Whitney U test.

Statistical Analysis

iPOND densitometry data are represented as mean ± SEM over at least 3 independent experiments. Fiber assay, Ub-AMC and Ub-CHOP2-Reporter data are represented as mean ± SD or mean ± SEM in one representative experiment and repeated at least 3 times unless otherwise indicated. Significance was determined by Student's t test and calculated using the Graphpad Prism software unless otherwise stated.